Optimization of scalaBle rEaltime modeLs and functIonal testing for e-drive ConceptS

EUROPEAN COMMISSION
Horizon 2020
GV-07-2017
GA # 769506

Deliverable No.	OBELICS D7.9	
Deliverable Title	Analysis of second life battery market, performances/aging and applications	
Deliverable Date	2020-11-30	
Deliverable Type	REPORT	
Dissemination level	Public (PU)	
Written By	Edoardo Locorotondo (UNIFI) Lorenzo Berzi (UNIFI) Luca Pugi (UNIFI)	2020-07-16 2020-07-16 2020-07-16
Reviewed by	Mohamed El Baghdadi (VUB) Luca Marengo (CRF) Alberto Reatti (UNIFI)	2020-11-20 2020-11-20 2020-11-20
Approved by	Horst Pfluegl (AVL) – Project Coordinator	2020-12-01
Status	Final	2020-12-01

Change log:

No.	Who	Description	Date
1	Edoardo Locorotondo	Creation of D7.9 Report & setting the structure of the document	17/06/2020
2	Luca Pugi	Input to the introduction	23/06/2020
3	Edoardo Locorotondo	Input to the Section 4.2 (complete)	02/07/2020
4	Edoardo Locorotondo	Input to the Section 6.2 (complete model of mobile network power consumption)	07/07/2020
5	Edoardo Locorotondo	Input to the Section 8.3 (complete)	16/07/2020
6	Lorenzo Berzi (UNIFI)	Input to the section 6	20/09/2020
7	Silvia del Pero (UNIFI)	Input to the section 9	10/10/2020
8	Luca Pugi (UNIFI)	Input to the section 6	15/10/2020
9	Lorenzo Berzi (UNIFI)	Wrap up and content organization	13/11/2020
10	Lorenzo Berzi (UNIFI)	Content update	22/11/2020
11	Lorenzo Berzi (UNIFI)	Content update	27/11/2020

Contents

Contents 3

Figures 4

Tables 5

Publishable Executive Summary 7

1.1 Document Structure 8

1.2 Deviations from original Description in the Grant Agreement Annex 1 Part A 8

1.2.1 Description of work related to deliverable in GA Annex 1 – Part A 8

1.2.2 Time deviations from original planning in GA Annex 1 – Part A 8

1.2.3 Content deviations from original plan in GA Annex 1 – Part A 8

2 Introduction 9

3 Second life battery market 12

3.1 Motivation for second life battery introduction 13

3.2 Boundary conditions for the proposed study 14

3.3 References for the present chapter 14

4 Evaluation of Li-ion batteries performances and aging parameters 15

4.1 Battery model in the second life 15

4.1.1 Introduction to modeling activities 15

4.1.2 Battery model 15

4.1.3 Aging model 18

4.1.4 Characterization tests and model parameters extraction 18

4.1.5 Model validation 20

4.1.6 Aged cells models: final considerations 22

4.2 References for second life cells model applications 22

5 Development of a methodology to link the appropriate second life battery to applications (grid, household, renewable) 24

5.1 Energy from the grid: linking environmental and economic cost 24

5.2 Chapter references 26

6 Definition of suitable case studies 27

6.1 The use of second-life battery as energy storage in tramway station: analysis, modeling, and simulation 27

6.1.1 Proposed Benchmark Test Case and Corresponding Implementation of the Model 27

6.1.2 Simplified Simulation Scenario: Simulation and Results 28

6.2 The use of second-life battery as energy storage in mobile network station: analysis, modeling, and simulation 31

6.3 Energy consumption model 32

6.3.1 Model validation: simulation results 35

6.4 Energy generation model 38

6.5 Energy management strategy 38
6.6 Full Model definition 39
6.7 Conclusions on the case study 41
6.8 References for the case study 41
7 Identification of possible scenarios for battery technology evolution 43
7.1 Characteristics of Battery Management Systems for system integration 43
7.1.1 Standard communication approach based on CANopen data 45
7.2 State of health (SOH) diagnosis based on impedance spectroscopy 46
7.2.1 Brief Description 46
7.2.2 State of the art of SOH monitoring methods 46
7.2.3 Battery electrochemical impedance spectroscopy (EIS) 47
7.2.4 Experimental EIS test description 48
7.2.5 EIS results 49
7.2.6 Conclusions 50
7.3 Chapter references 51
8 Life cycle assessment of second life batteries (LCA) 53
8.1 Production impact of Lithium batteries 53
8.2 Production impact of other battery type alternative to second-life battery 54
8.3 Repurposing and Recycling impact 54
8.4 Use phase 56
9 Conclusions on second life battery applications 58
10 Acknowledgement 59

Figures

Figure 3-1: Expected EV stock according to different scenarios in Europe [1] 12
Figure 3-2: Market growth of subcomponents for battery production [2] by sector. 12
Figure 4-1: Battery model based on EEC circuit 15
Figure 4-2: Battery voltage model by using EEC 16
Figure 4-3: Battery aging model implementation to assess SOH during the use 18
Figure 4-4: Open circuit voltage (on the left) and internal resistance (on the right) evaluation for the NMC under test at different SOC and SOH during the charging/discharging phase 19
Figure 4-5: Resistances of RC-blocks evaluation for the NMC under test at different SOC and SOH during the charging/discharging phase 20
Figure 4-6: Capacitances of RC-blocks evaluation for the NMC under test at different SOC and SOH during the charging/discharging phase 20
Figure 4-7: Layout of the Simulink NMC second life battery model and parameters setup 21
Figure 4-8: Pulse discharging and charging test: comparison between experimental and simulation voltage data 21
Figure 4-9: Pulse discharging and charging test: absolute error comparison between experimental and simulation voltage data 21
Figure 5-1: Carbon intensity variability of electric energy generation in Italy depending on day hour and year period. Data have been processed from Italian grid manager source [1]. Lines represent 24 typical days (per each of the 12 months, one weekend and one weekday value have been plot). 25

Figure 5-2: Energy cost in €/kWh per hour of the year (0-8760) on the Italian market. 25
Figure 5-3: Aggregated environmental and economic normalized cost, obtained using weighting factors both equal to 0.5. 26
Figure 6-1: Benchmark test case Sirio-Firenze Tramway 27
Figure 6-2: simplified scenario adopted for simulation 28
Figure 6-3: Example of constrained mission profile (max speed 45 kmh, max acc. ±1ms-2, max jerk ±0.4ms-3) 29
Figure 6-4: energy consumptions (left) as function of power station configurations and kd, voltage V2 collected by the second Tram as function of kd (on right) 29
Figure 6-5: relative energy consumptions with conventional single quadrant substations (a), with ideal reversible power stations (b), with a storage that has an equivalent efficiency of 0.8, losses with different equivalent copper sections of the line 30
Figure 6-6: energy consumption respect to speed and kd with single quadrant powerstations (a), and with reversible power stations (b), supposed storage eff. 0.8 30
Figure 6-7: The mobile access network plant 31
Figure 6-8: MIMO transmit antennas model [10] 32
Figure 6-9: Normalized traffic per different days and use scenarios 33
Figure 6-10: Backhauling layout considered in [13]; in this work, we consider only micro cell BSs. 35
Figure 6-11: Layout of the Simulink mobile network power consumption model and parameters setup 37
Figure 6-12: Day profile model of mobile network in an Urban area of 40 km2: (a) Traffic demand (b) Power net consumption (c) Number of ON base stations 37
Figure 6-13: Business scenario, Dense Urban area: AEE as a function of (a) covered area ($\boldsymbol{NTX = 2}$) and of (b) number of transmit antennas ($\boldsymbol{A = 40\ km2}$) 37
Figure 6-14: PV capacity factor variation over season and hour. 38
Figure 6-15: System structure layout. All peripherals share the DC-bus connection. All data are acquired by a power control unit which commands zero/positive/negative DC current from bidirectional AC/DC converter. 39
Figure 6-16: Layout of Matlab/Simulink model, including main subsystems such as: A) PV generation unit; B) Energy management and conversion unit; C) RB unit and energy consumption estimation; D) Battery derived from automotive case study, including efficiency, SOC and SOH assessment. 39
Figure 6-17: Expected energy balance (upper figure) and scheduled power requested from grid. 40
Figure 6-18: GHG emissions for RB case study, with PV, with PV and battery. 41
Figure 6-19: Energy cost for RB case study, with PV, with PV and battery. 41
Figure 7-1: typical use of battery system according to [1]. BMS is communicating with other control systems installed in the destination plant. 44
Figure 7-2: Reference spectrum of lithium battery in a wide frequency range and battery EIS modeling. 47
Figure 7-3: Sequence of EIS tests performed on an aged cell, interspersed by CC discharging at C/2 and rest time of 30 mins 49
Figure 7-4: Measured battery impedance (SOH=60%) at various SOC: (a) Nyquist diagram, (b) SEI resistance and charge-transfer resistance evaluation 49
Figure 7-5: Battery impedance curve for NMC cell at different SOH (fixed SOC=60%) 50
Figure 7-6: Resistance parameters extraction for EOL NMC cells at different SOC and SOH 50
Figure 8-1: Energy flows of the system (Bobba et al.) 56
Figure 8-2: System boundary to compare environmental implications of battery choice for stationary energy storage (Richa et al.) 57

Tables

Table 2-1: Storage Specifications 9
Table 2-2: Application Features 10
Table 2-3: Application Features 10
Table 2-4: Evaluation of Proposed Feasibility Indexes for both proposed applications 10
Table 3-1: Potential market applications of repurposed Li-ion batteries [3]. 13

Table 4-1: Battery cells under test at different SOH 19
Table 6-1. Main features of modelled Hitachi Sirio-Firenze Tramway 27
Table 6-2. Simplified Feature of Line Considered for Sirio Firenze Line 28
Table 6-3. Typical traffic for various area type. 31
Table 6-4: List of parameters 35
Table 6-5: Resulting traffic peak demand for different area type for the year 2020 36
Table 6-6: Parameters adopted for model sizing 40
Table 7-1: Historical data to be stored on the BMS for repurposing diagnostics 44
Table 7-2: Data to be exchanged between BMS and plant during in-life service: proposal of a minimal set. 45
Table 8-1: Production impacts for different Li-ion batteries 53
Table 8-2: Production impacts for Pb batteries 54
Table 8-3: Production and repurposing impacts for different Li-ion batteries 54
Table 8-4: Production and end of life impacts for different Li-ion batteries 55
Table 8-5: End of life impacts for Pb batteries 56
Table 8-6: Energy flows for the reference and the repurposed scenarios (Bobba et al.) 56

Publishable Executive Summary

State of the art

In the automotive applications and in particular for battery electric vehicles, the cost of the battery systems is still very high (mainly 1/3 of the vehicle cost), which is one of the barriers for a high market penetration. In order to reduce the cost, the battery systems for powering the electric vehicles (i.e. PHEV, HEV and BEV) also can be used for stationary applications after end of life. Basically, there are two ways to use vehicle's battery system for grid applications:

1. Vehicle-to-grid (V2G) application utilizes the battery for grid services, whereas the battery is still in the vehicle;

2. Reuse battery systems after retiring from vehicular services for stationary applications to reduce the TCO.

Challenges

Second-life batteries are still expected to be capable of storing, delivering substantial energy and to meet the requirements of stationary applications. However, the total lifetime value of the battery will increase when the remaining capacity of batteries can be invested to meet the requirements of other energy-storage applications. Consequently, the price of battery systems will be decreased and thus the TCO of the BEV will decrease, which helps to widespread commercialization both of electric vehicle and grid battery systems. However, there is an increasing need to investigate in depth the potential of using second-life batteries for stationary applications (i.e. electric supply, ancillary services, grid system, end user/utility customer and renewables integration). One of the key challenges related to second life batteries is that the battery behavior and in particular the aging phenomenon after first life are not clearly known for the different battery chemistries. Therefore, there is a lack of reliable and accurate battery models to assess the applicability of batteries from BEV into stationary applications.

Progress beyond the state of the art

In OBELICS, UNIFI with the support of VUB will use their expertise in the field of battery assessment, testing and modelling to evaluate the behavior of the battery system after first life for stationary applications as an input to define clear cases where second life batteries can be used and to which level. In particular the unique VUB database of battery aging during first and second life will be used as a starting point to develop reliable battery models to evaluate the suitability of this technology for second life applications. The main focus will be to reduce the TCO and to have a better sizing of the battery system.

Innovation potential

To our knowledge such extended database and reliable battery models during second life do not exist yet.

1. Purpose of the document

The purpose of this document is to provide an overview on second life battery applications, which is an activity mainly related to Task 7.3 “Analysis of second life battery market, performances/aging and applications”. Battery characterization examples, case studies for second life battery installation and environmental impact considerations are included.

1.1 Document Structure

Main sections of the document are reported here. The aim of the Deliverable 7.9 is to provide a quite enlarged overview on second life applications for batteries considering the market opportunities, the potential applicability to certain case studies – modeled here in the document – and the environmental and economic impact considerations related to the applications. Therefore, it can be said that case studies (support to railway vehicles; support to telecommunications systems) are central for such deliverable.
A multidisciplinary approach has been necessary to perform the whole activity since it included various phases requiring different tools and competencies, from battery testing to system modelling, from Life Cycle Assessment competencies to system control applications. At the end of each chapter, the reader can find the reference list relevant for that chapter. The document is structured as follows:

1. This section: purpose of the document
2. Introduction to second life battery applications
3. Considerations on second life battery market
4. Evaluation of Li-ion batteries performances and aging parameters
5. Development of a methodology to link the appropriate second life battery to applications
6. Definition of one or more suitable case studies and analysis of related business models
7. Identification of possible scenarios for battery technology evolution
8. Life cycle assessment of second life batteries (LCA)
9. Final remarks

1.2 Deviations from original Description in the Grant Agreement Annex 1 Part A

1.2.1 Description of work related to deliverable in GA Annex 1 – Part A

Task 7.3: Analysis of second life battery market, performances/aging and applications (UNIFI, VUB) [M1-36]

- Analysis of second life battery market (technical/economical),
- Evaluation of li-ion batteries performances and aging parameters based on VUB database/models,
- Development of a methodology to link the appropriate second life battery to applications
- Definition of one or more suitable case studies and analysis of related business models
- Cost comparison with technologies suitable for energy storage application (e.g. Lead Batteries, LiFePO4)
- Identification of possible scenarios for battery technology evolution (e.g. on a 10-year basis) and proposal of guidelines for system upgrading and BMS design guidelines.
- Life cycle assessment of second life batteries (LCA)
- Environmental Life Cycle Assessment for main case-studies comparison
- Economic Life Cycle Costing and/or suitable business model build up

The proposed task will enable to reduce the development and testing effort.
In addition, the LCA and LCC will allow to assess the reliability, energy content and commercial certainty for battery systems at all levels of technology, from cell via packs, vehicles to recycling. VUB will support with analysis of the behavior of second life batteries coming from EVs, HEVs and LCA and LCC activities.

1.2.2 Time deviations from original planning in GA Annex 1 – Part A

There are no deviations with respect to the timing of this deliverable.

1.2.3 Content deviations from original plan in GA Annex 1 – Part A

There are no deviations from the Annex 1 – Part A with respect to the content.

2 Introduction

Reuse of reconditioned Second Life Batteries from Automotive Market offers interesting opportunities in terms of improved environmental impact of electric storage systems also boosting the infrastructural growth which is needed to sustain and boost the diffusion of electrical mobility.
In order to properly evaluate the applicability of 2nd life storage systems to real industrial applications, specification regarding both storage (Table 2-1) and requirements of the chosen application (Table 2-2) should be considered. By crossing and comparing the two tables, it is possible to define the corresponding suitability indexes defined in Table III. Definition of these metrics are fundamental for the evaluation of a generic 2nd life application with respect to the corresponding features of the chosen 2nd life battery pack technology.
By defining five indexes as the ratio between corresponding ratios between Storage specification and chosen load features it's possible to roughly evaluate the feasibility of the proposed application for the chosen second life battery technology.
Once this five indexes are successfully evaluated there is a high probability that the chosen 2nd life storage should be well suited for the chosen application so a further final evaluation should be performed by comparing the application of the 2nd life storage system with a corresponding implementation performed with a conventional storage system both in terms of economic balance and equivalent environmental impact including a complete LCA analysis.
In these work there are two different applications considered:

- The first one is the application of 2nd life cells to storage//backup units for mobile network stations
- The second one is the application of 2nd life cells to ground based storage systems to improve the efficiency of high speed railway lines by installing some additional storage systems in order to optimize efficiency and performances of power stations that are used to feed the line.

For both proposed applications preliminary evaluation of the five indexes defined in table 3-3 clearly indicates the potential feasibility of 2nd life cells recovered from the automotive market as indicated in table 3-4

Table 2-1: Storage Specifications

Storage Specification (Acronym)	Note
Residual Performance (SRP)	Residual Performance of the storage system should be evaluated in terms of actualized Specific Power (W/kg or W/dm^3) and Specific Energy (Wh/kg or Wh/dm^3).
Residual Life (SRL)	Expected residual life should be evaluated in terms of residual specific ampere-hour throughput (C/kg or C/dm^3) evaluated with respect to residual specific power.
Reliability/Traceability (SRT)	Expected Failure Reliability Rate (statistical occurrence of a failure) that should be assured with an efficient tracing of the actual SOH of the battery including specific features of 1st life application on the original vehicle.
Observability Diagnostic and Prognostic (SO)	Availability of efficient online Prognostic and Diagnostic system to continuously evaluate the state of cells. Prognostic features are fundamental for a proper planning of maintenance activities (substitution of cells with short foreseen life). This index is quantified as the probability of detecting an incoming failure.
Redundancy (SRD)	System is designed to tolerate multiple cell failures and to make possible their easy substitution without compromising system availability. This index is quantified in terms of tolerated percentage of faulted//unavailable cells.

Table 2-2: Application Features

Load Specification (Acronym)	Note
Required Performance (LRP)	Required specific performance in terms of Specific Power (W/kg or W/dm^3) and Specific Energy (Wh/kg or Wh/dm^3). This index takes count not only of load features but also of admissible weights and encumbrances for chosen applications.
Required Life (LL)	Desired residual life should be evaluated in terms of residual specific ampere-hour throughput (C/kg or C/dm^3).
Required Reliability (LRR)	Desired Failure Reliability Rate (statistical occurrence of a failure).
Req. Observability (LO)	This index is quantified as the desired probability of detecting an incoming failure of the storage.
Redundancy (LRD)	This index is quantified in terms of required robustness evaluated in terms of percentage of faulted/unavailable elements to which system has to survive.

Table 2-3: Application Features

Relative Suitability Index	Definition
$P_{RP} = \frac{SRP}{LRP}$	A high value implies that residual performances of battery are quite higher with respect to expected ones.
$P_L = \frac{SRL}{LL}$	A high value implies that residual life of the battery is far enough with respect to the desired one for the chosen application.
$P_R = \frac{LRR}{SRL}$	A high value implies that the occurrence of a failure of the storage is relatively low with respect to desired reliability for the chosen application.
$P_O = \frac{SO}{LO}$	A high value of the index indicated that it is relatively simple to foresee and prevent an incoming failure or degradation of the storage respect to a specified level that is considered as satisfying for the proposed application.
$P_D = \frac{SRD}{LRD}$	A high value implies that storage is substantially much more fault tolerant with respect to load specifications in terms of fault mitigation.

Table 2-4: Evaluation of Proposed Feasibility Indexes for both proposed applications

Relative Suitability Index	Mobile Network Stations	Railway Storage Systems
$P_{RP} = \frac{SRP}{LRP}$	**HIGH:** It's a static application in which relatively high encumbrances of the storage system are well tolerated. Battery has to work	**HIGH:** It's a static application so high encumbrances are well tolerated. Stored energy is relatively modest , design is substantially constrained by

	only as backup unit with modest requirements in terms of specific power and energy.	the size of peak powers associated to regenerative braking and traction of trains.
$P_L = \frac{SRL}{LL}$	HIGH: Proposed application regards as backup unit so usage is not frequent, in terms of required residual life of cells quantified as current throughput is modest.	HIGH In proposed application storage design is mainly constrained by considerations regarding tolerated peak power, that leads for 2nd life cells to relatively cautious designs in terms of stored energy. So residual life in terms of residual current throughput is relatively high.
$P_R = \frac{LRR}{SRL}$	HIGH: Statistical Occurrence of the load application is relatively low so it's not difficult to assure the overall reliability required by the application.	HIGH: It's not required to have a very high reliability rate of the storage since a failure of the storage affects efficiency but not safety or reliability of the railway service.
$P_O = \frac{SO}{LO}$	HIGH For most of the operational life proposed backup storage should be idle, so there is the possibility of implementing time consuming diagnostic features based for example on spectroscopy and or FRF response analysis to monitor the pack. Also, the storage is connected to mobile network so complex remote prognostic procedures are relatively easy to be implemented.	HIGH Storage is installed as a complementary system of railway power stations which are continuously monitored so it's relatively easy to do the implementation of remote prognostic and diagnostic procedures.
$P_D = \frac{SRD}{LRD}$	**HIGH** It's possible to obtain a relatively high redundancy of the system with a modular design that allows the fast substitution of submodules.	**HIGH** It's possible to obtain a relatively high redundancy of the system with a modular design that allows the fast substitution of submodules.

3 Second life battery market

Automotive market is under rapid evolution and recent forecasts [1] suggest that a significant stock of electric vehicles (depending on the policy) is expected by 2030 (see Figure 3-1); in parallel, a growth of other technological sectors potentially using relevant amount of battery cells is also expected (see Figure 3-2). In other words, a worldwide growth in Li-based battery adoption is undoubted. These data suggest that battery exchange on the market will be driven by aspects such as:

- A strong request of battery cells for new products, with automotive sector being relevant worldwide due to sensitiveness for environmental impact reduction and need for energy transition
- Following a few years delay, the need for proper End Of Life options for used batteries, which include
    - Reuse
    - Recycling

Assuming that battery life is necessarily limited by material degradation, the objective of reuse applications is to prolong life on a time-limited scenario for which the battery is still sufficiently efficient and reliable. The more opportunities are provided for reuse, the later occurs the need for recycling, which is certainly the final destination for all cells on a 15-20 years perspective.

In case of appropriate methodologies for collocation on the market of second life batteries, therefore, reuse can be not only a solution to avoid the production of new cells (therefore limiting the extraction of new materials), but it can also guarantee proper energy storage devices on the market at reduced cost and large availability, thus reducing competition with the automotive sector.

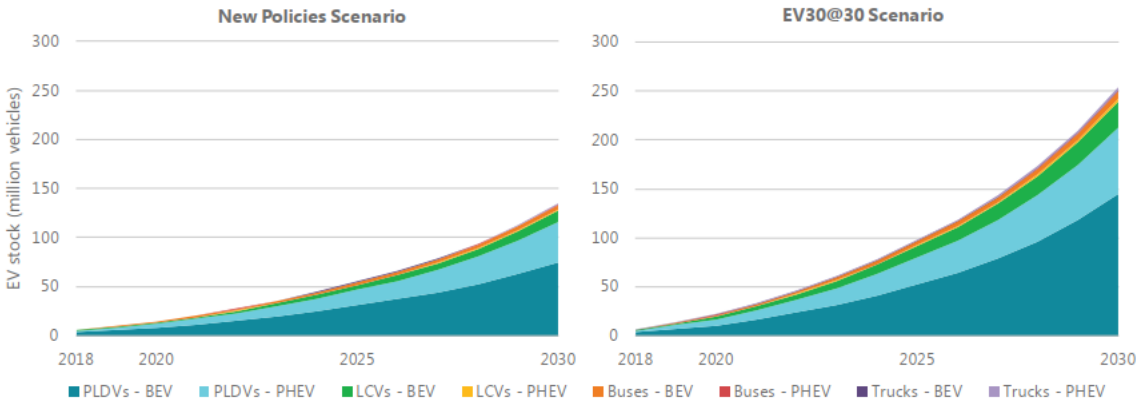

Figure 3-1: Expected EV stock according to different scenarios in Europe [1]

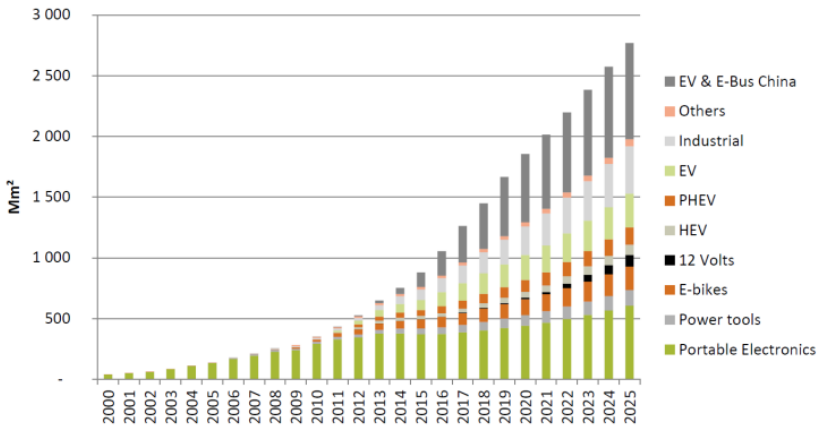

Figure 3-2: Market growth of subcomponents for battery production [2] by sector.

Looking at potential adopters for second life batteries, Table 3-1 suggests that most applications of second life batteries should be for stationary use and that a potential use of millions of batteries is expected worldwide.

Table 3-1: Potential market applications of repurposed Li-ion batteries [3].

Market application	Number of repurposed packs	Estimated market size	Cycle frequency	Potential for application	Limitations for application
Residential	1-2	> 3 Million'	Daily	- Large market - Small, easy-to-handle units - Market can be incrementally developed	-Regulated pricing minimizes savings for user - Risk and maintenance must be addressed
Telecommunication towers	5-10	100,000 s	Daily and back-up	- Motivated for onsite energy storage, and back-up currently has many sites	- High reliability demanded by application, and would be difficult to achieve
Light commercial	10-15	10,000-100,000	Daily	- Greater savings due to unregulated electricity pricing - Availability of expertise, location, and personnel to support the technology	- Safety regulations for storing batteries on site must be determined - More packs are required
Office building	30-40	100,000	Daily	- Greater savings due to unregulated electrical pricing - Can complement generator use	- Larger application requires significant storage investment - Urban locations may create greater risks
Fresh food distribution centers	30-40	10,000-100,000	Daily	- Greater savings due to unregulated electrical pricing - Large electrical demand with highly controllable equipment will work well with technology - Possibility of attracting early adopters if business case can be demonstrated - Have the expertise, location and personnel to support the technology	- Larger application requires significant storage investment - Payback must be clearly demonstrated
Stranded power (renewables)	900	Uncertain (< 10)	10-20/Month	- Intermittent nature of renewable energy justifies energy storage - Availability of expertise, location and personnel to support the technology - Motivated early adopters allow for greater market penetration of wind and solar	- Size of application may use up supply or the supply will not be available - Increased risk of fire - Complexity of controlling packs of varying states of health
Transmission support	1000 s	Uncertain (<10)	1/Months	- Large energy needs create larger market for batteries - Currently users of auxiliary electricity services and thus have some comfort with the application	- Size of application may use up supply or the supply will not be available - Increased risk of fire
				- Motivating early adopters to help ease transmission congestion. - Benefits can be achieved even if worked with smaller market and customers base.	- Complexity of controlling packs of varying states of health

3.1 Motivation for second life battery introduction

Second life battery applications have been proposed in quite wide literature reports in the last decades, and are based on the assumption that significant performances are still available for such batteries even if their capacity, power or reliability indicators make them unfit for the automotive use.

Main motivations for second life battery implementation are:

- Large scale production and technical improvement for automotive Lithium batteries provide improvement of the energy storage system. It is possible that existing EV batteries will be replaced not only for degradation, but mainly for obsolescence in comparison with newest models.
- The cost of battery systems is still very high: for automotive applications, mainly 1/3 of the vehicle cost is related to it, while for other applications investment cost can discourage battery installation.
- In order to reduce the cost, the battery systems for powering the electric vehicles (i.e. PHEV, HEV and BEV) also can be used for stationary applications after end of life (EOL).

- Lithium battery is “end of life” if at 85-80% rated capacity, in automotive applications; such degraded performance can still be acceptable for other uses:
    - Second-life batteries are still expected to be capable of storing, delivering substantial energy and to meet the requirements of stationary applications.

Main challenges identified for second life applications are:

- Performance assessment:
    - Evaluation of Energy Loss due to battery efficiency degradation, in particular it is necessary identify under which boundary conditions (e.g. temperature, C-rate, SOC) the performance is sufficient to provide an economic and/or environmental advantage
- Evaluation of **Credit Value** (in terms of *economical cost* and *environmental impact*) due to replacement it to the current supply systems.
- Identification of reliable and accurate aged battery models to guarantee correct performance prevision in application models and to obtain sufficient forecast for battery durability.
- Identification of technological barriers (e.g. communication standards) for integration in the selected applications; the more barriers are present, the more effort and cost are required for battery repurposing.

3.2 Boundary conditions for the proposed study

Considering preliminary literature studies, internal meetings between OBELICS partners have been set in order to define those conditions under which the virtual applications can be assessed considering the real-world context. Main assumptions are summarized as follows:

- Attribution of battery environmental impact attribution to 1st and 2nd life:
    - Partners assumed it to be Independent, so that 2nd life follows 1st life without modifying or shortening the automotive use for which the energy storage is built. As a consequence, only second life impact will be assessed.
- Repurposing impact:
    - Battery re-use implies dismantling from vehicle, collection, implementation of new functionalities (e.g. module dismantling and reassembly or as-is installation) and transportation to the place of use. Such assessment will be done according to literature examples.
- Repurposing «Credit»
    - The credit related to the substitution of new produce will be assessed considering battery technologies alternative for the selected applications, which are not necessarily of the same typology (eg. 2nd life Li-ion batteries may substitute lead batteries or other Li-based cells, if they are a reference benchmark typical for that application).
- In use credit will be assessed according to effective duration forecast, according to suitable ageing models.

3.3 References for the present chapter

[1] International Energy Agency, *Global EV Outlook 2019: Scaling-up the transition to electric mobility*. OECD, 2019.

[2] N. Lebedeva, F. D. Persio, e L. Boon-Brett, «Lithium ion battery value chain and related opportunities for Europe», Publications Office of the European Union, Luxembourg, EUR 28534 EN, 2017.

[3] E. Hossain, D. Murtaugh, J. Mody, H. M. R. Faruque, M. S. H. Sunny, e N. Mohammad, «A Comprehensive Review on Second-Life Batteries: Current State, Manufacturing Considerations, Applications, Impacts, Barriers Potential Solutions, Business Strategies, and Policies», *IEEE Access*, vol. 7, pagg. 73215–73252, 2019, doi: 10.1109/ACCESS.2019.2917859.

4 Evaluation of Li-ion batteries performances and aging parameters

Considering the peculiarities of second life cells, only limited literature is available on the performance assessment and their modelling activities after significant degradation occurred. Due to this reason, the target of the partners involved in such activity has been to assess the performance and aging parameters.

4.1 Battery model in the second life

4.1.1 Introduction to modeling activities

In this section, we analyze the performance, in terms of energy stored and power availability, of an automotive Li[NiCoMn]O_2-based Cathode type (briefly called NMC) pouch cell, having a nominal capacity of 20 Ah [1]. Specifically, we tested four NMC cells at different State-Of-Health (SOH) and considered at End-Of-Life (EOL), so ready for possible second use. The characterization tests, which we considered, are according to the battery standard tests described in the previous OBELICS works (cf. D7.2, D7.5). These tests are the most important towards the modeling of a second life battery model, analysis of the performances, and the aging. The scope of this section is to provide as much information as possible about battery performance after EOL. To achieve this scope, the second life battery virtual model, with aging property, is realized and implemented in Matlab/Simulink. The battery model is based on an electrical equivalent Thevenin circuit, of which the parameters are extracted by an appropriate parameter identification algorithm during the characterization tests. Hence, this section provides a battery performance model that could be simply built in some simulation platforms, analyzing battery second use in some less-demanding applications, where reduced performance is still acceptable.

4.1.2 Battery model

Exciting the battery with discharging or charging current, the battery model, which simulates the battery voltage response, is based on an electrical equivalent circuit (EEC) represented in Figure 4-1.

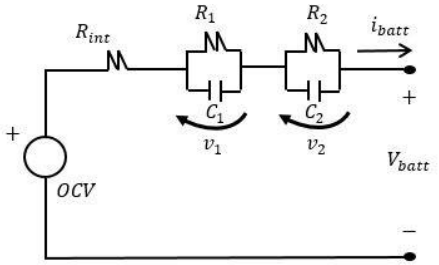

Figure 4-1: Battery model based on EEC circuit

Battery model, used in this section, is composed by the series of the following circuit elements:

- **Open Circuit Voltage (*OCV*):** is defined as the voltage measured between terminals of the cell at rest since a certain period (depending on the stabilization of the voltage) with no load connected to it.
- **Internal resistance (R_{int}):** is defined by the instantaneous battery drop voltage response to step input current.
- First RC group (R_1, C_1): battery has ohmic-capacitive behavior after an input discharging/charging current pulse, hence, battery voltage increase/decrease during the rest period (voltage relaxation) until it reaches the corresponding OCV. Usually, battery voltage relaxation is defined by two time-constants. The first RC group simulates the voltage relaxation with the fast time constant.
- Second RC group (R_2, C_2): simulates voltage relaxation with a slow time constant. Usually, no more than two RC blocks are adopted for real-time application and battery model simulations.

The mentioned circuit parameters accurately simulate the battery voltage, considering an input pulse current, as depicted in Figure 4-2.

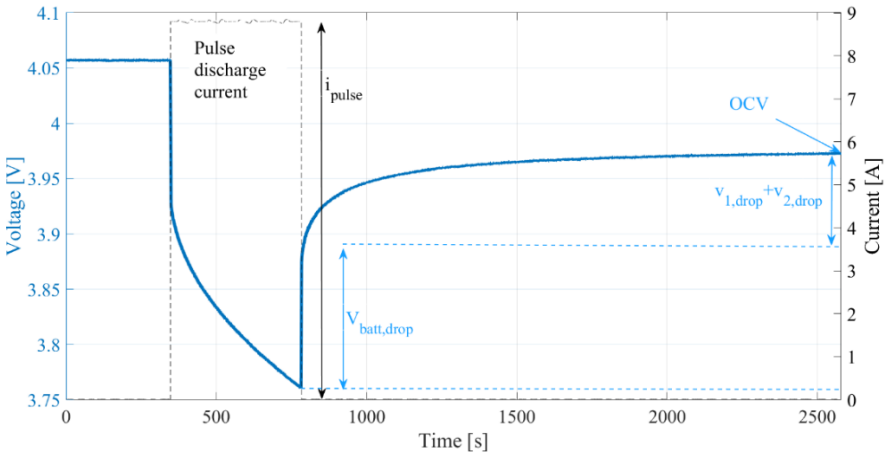

Figure 4-2: Battery voltage model by using EEC

Referring to the EEC model depicted in Figure 4-1 and considering the time constant $\tau_i = R_i C_i$, battery voltage evolution is described by the following discrete-time difference equations system, with the time integer index *k* and the sample time *T*:

$$\begin{cases} v_{1,k+1} = v_{1,k} e^{-T/\tau_1} - R_1 i_{batt,k} (1 - e^{-T/\tau_1}) \\ v_{2,k+1} = v_{2,k} e^{-T/\tau_2} - R_2 i_{batt,k} (1 - e^{-T/\tau_2}) \\ V_{batt,k} = OCV_k - v_{1,k} - v_{2,k} - R_{\text{int}} i_{batt,k} \end{cases}$$

Equation 4-1

The battery model (Equation 4-1) is similar to a Linear and Time-Invariant (LTI) system. However, an accurate battery model should have several non-linear properties, also circuit parameters are time-varying. The battery is a non-linear model due to the OCV dependency by the State Of Charge (SOC) with a non-linear relationship. The OCV-SOC curve has usually a linear trend in the middle of the battery SOC window and an exponential trend at the extreme of the SOC window. Moreover, especially for LiFePO4 cathode type, there is a noticeable OCV difference between charging and discharging curves, due to the hysteresis behavior which the battery has [4]. As just said, circuit parameters of battery model (Equation 4-1) depend on the current battery operating condition: many internal/external factors affect the circuit parameters values, such as SOC variations, the sign of the current variations (charging/discharging phase) and rate of load current [6], temperature variations [7], and, finally, the age of the battery [8]. UNIFI realized a battery model based on EEC considering the non-linear behavior of the OCV just cited and the variation of circuit parameters value with SOC, the sign of the input current, and the aging variations. Therefore, referring to (Equation 4-1), the mathematical battery model is transformed to the following non-linear and time-variant (NLTV) dynamic system:

$$\begin{cases} OCV = g(SOC_k, SOH_k, sign(i_{batt,k})) \\ [R_{\text{int}}, R_1, R_2, C_1, C_2] = [f_{R_{\text{int}}}, f_{R_1}, f_{R_2}, f_{C_1}, f_{C_2}](SOC_k, SOH_k, sign(i_{batt,k})) \\ v_{1,k+1} = v_{1,k} e^{-T/\tau_1} - R_1 i_{batt,k} (1 - e^{-T/\tau_1}) \\ v_{2,k+1} = v_{2,k} e^{-T/\tau_2} - R_2 i_{batt,k} (1 - e^{-T/\tau_2}) \\ V_{batt} = OCV - v_{1,k} - v_{2,k} - R_{\text{int}} i_{batt,k} \end{cases}$$

Equation 4-2

In this model, we neglect the dependence of the OCV and impedance parameters by temperature variations. The set of the parameters $[OCV, R_{int}, R_1, C_1, R_2, C_2,]$ is calibrated offline under lab tests with entire SOC interval [0;100]%, in the charging/discharging phase, and at a different age, identified by the State-Of-Health indicator. The SOC is calculated by using the classical Ampere-Counting method:

$$SOC_{k+1} = \left[SOC_k - \frac{i_{batt,k} T}{3600 \times C_{curr}} \right] \times 100$$

Equation 4-3

Where C_{curr} is the battery capacity evaluated with a standard cycle during the capacity test [2]. Battery SOH, as defined in [9], is a metric to evaluate the aging level of batteries, which often includes capacity fade and/or power fade. Despite there are different to assess battery SOH value, in this section the SOH parameter is the comparison of the current evaluated capacity with standard cycle respect to the initial capacity.

$$SOH = \frac{C_{curr}}{C_{nom}} \times 100$$

Equation 4-4

Where C_{nom} is the nominal capacity of the battery at the beginning of life. According to Equation 4-4 battery, current capacity C_{curr} assesses the battery SOH, which, in this section, denotes the battery age. The battery is considered in the EOL if at 85-80% of the nominal capacity, hence $SOH = [85 \div 80]\%$. Current research works verified the possibility to consider the cycle second life of lithium battery starting from 85-80% of SOH until 60% [10] or 50% [11]. To complete the EEC battery model (Equation 4-2) with SOC (Equation 4-3) and SOH (Equation 4-4) calculation, an aging model is identified by experimental data. In this section, the battery current capacity C_{curr} depends on the Ampere-hour throughput parameter Ah_{thr} and the depth of discharge (DOD).

$$C_{curr} = f_{cyc}(Ah_{thr}, DOD)$$

Equation 4-5

The Ampere-hour throughput represents the total energy, in Ah, that was delivered and stored by the battery during its current cycle life. It's calculated by the following equation:

$$Ah_{thr,k+1} = Ah_{thr} + \frac{T|i_{batt,k}|}{3600}$$

Equation 4-6

The DOD parameter denotes the fraction of the capacity discharged from the fully charged battery. Finally, the complete battery model, with aging is according to the differential equations system:

$$\begin{cases} Ah_{thr,k+1} = Ah_{thr,k} + \dfrac{T\,|\,i_{batt,k}\,|}{3600} \\ C_{curr,k} = f_{cyc}(Ah_{thr,k}, DOD) \\ SOH_k = \dfrac{C_{curr,k}}{C_{nom}} * 100 \\ SOC_{k+1} = (SOC_k + \dfrac{T * i_{batt,k}}{3600 * C_{curr,k}}) * 100 \\ \\ OCV = g(SOC_k, SOH_k, sign(i_{batt,k})) \\ [R_{\text{int}}, R_1, R_2, C_1, C_2] = [f_{R_{\text{int}}}, f_{R_1}, f_{R_2}, f_{C_1}, f_{C_2}](SOC_k, SOH_k, sign(i_{batt,k})) \\ v_{1,k+1} = v_{1,k} e^{-T/\tau_1} - R_1 i_{batt,k}(1 - e^{-T/\tau_1}) \\ v_{2,k+1} = v_{2,k} e^{-T/\tau_2} - R_2 i_{batt,k}(1 - e^{-T/\tau_2}) \\ V_{batt} = OCV - v_{1,k} - v_{2,k} - R_{\text{int}} i_{batt,k} \end{cases}$$

Equation 4-7

As mentioned, all the model parameters were identified by experimental tests. Details on the battery aging model (Equation 4-5) are shown in the next subsection.

4.1.3 Aging model

Eight NMC pouch cells of the same manufacturer, previously cited, have been cycled until they have reached EOL and went beyond it. The cells were subjected to 8 different cycle life tests, composed by constant-current (CC) and, finally, constant-voltage (CV) charging (0.5C, where C is nominal capacity); followed by discharging phases, interspersed with pauses, at a room temperature of 35°C.

A summary of these cycle life tests and more details about the battery's history is depicted in [12].

Cycle life tests were carried out in ENEA research center from 2015 to 2018. Afterward, the cells have not been used for about 2 years, and have been stored in the same conditions (in a not thermally controlled environment). Figure 4-3 depicts the amount of the total energy of the NMC battery under test at different DODs, considering the cycle life test cited above, where the discharging phase is characterized by a constant current with a rate of discharge 1C (20 A). We infer by Figure 4-3 that the amount of energy, which the battery can use during its cycle life, increases when the DOD decreases. Moreover, in the same Figure, the dash lines track the total energy which can be used by the battery during the second life, considering the range of SOH in $[80 \div 50]$.

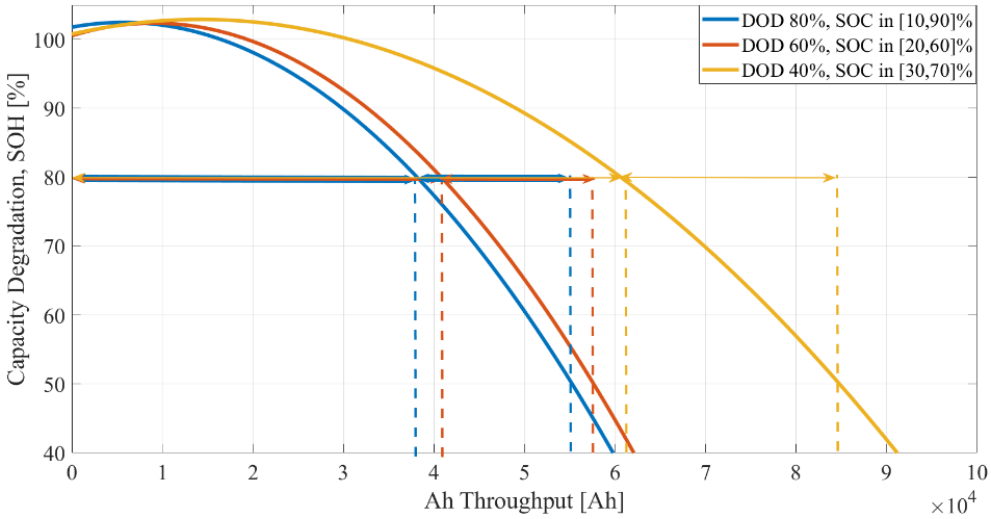

Figure 4-3: Battery aging model implementation to assess SOH during the use

4.1.4 Characterization tests and model parameters extraction

Four of the eight EOL cells were tested in the UNIFI laboratories during the period 2019-2020. Following the battery characterization test procedures described in the previous deliverable of the OBELICS project [2][3], we perform the following test:

- **Preconditioning Test:** three full discharge/charge cycles at a fixed rate of discharge C/5, interspersed with a pause of 1h between discharging and charging phase.
- **Capacity Test:** three full discharge/charge cycles, maintaining a charging C-Rate of C/3 (first in CC mode, finally in CV mode), changing the discharge C-Rate of C/2, C/3, and C/4.
- **Pulse Test:** during the discharging phase, the battery is excited by a series of fourteen C/2 discharged current pulses, separated by 30mins of the rest period. Each pulse discharges the 7% of battery capacity until the lower threshold voltage is reached (3.0V). Then, during the charging phase, the pulse test is set as similar to the discharging phase, reaching the higher threshold voltage (4.15V) in CV mode.

The model parameters identification is based on the battery current and voltage measurement acquired during the test, using the laboratory test setup shown in [6].

During the capacity test, battery current capacity C_{curr} is evaluated at a different rate of discharge: a summary of the capacity estimated for the different 4 EOL cells is shown in Table 4-1.

Table 4-1: Battery cells under test at different SOH

Battery n.	Last capacity estimated [Ah]	State Of Health (4)
#3	16	80%
#4	17	85%
#5	12	60%
#8	10	50%

The OCV and the set of impedance parameters $[R_{int}, R_1, C_1, R_2, C_2]$ are identified during the discharging/charging pulse test. Referring to Figure 4-2, the OCV is obtained as the last voltage value acquired during voltage relaxation in the pulse test. The internal resistance parameter R_{int} is acquired from the sudden drop voltage $V_{drop,batt}$ due to current pulse i_{pulse}:

$$R_{int} = \frac{V_{batt,drop}}{i_{pulse}}$$

Equation 4-8

Finally, the two RC groups parameters $[R_1, C_1, R_2, C_2]$ are identified by fitting the voltage relaxation curve, as shown in Figure 4-2, recalling the following analytical equation:

$$OCV - V_{batt}(t) = v_{1,drop} e^{-t/\tau_1} + v_{2,drop} e^{-t/\tau_2}$$

Equation 4-9

The characterization tests are performed on the battery cells at different SOH shown in the Table 4-1, and results of the EEC battery model parameters identification are shown in the Figures 4-4 (OCV, internal resistance), 4-5 (resistances of RC blocks) and 4-6 (capacitances of RC blocks).

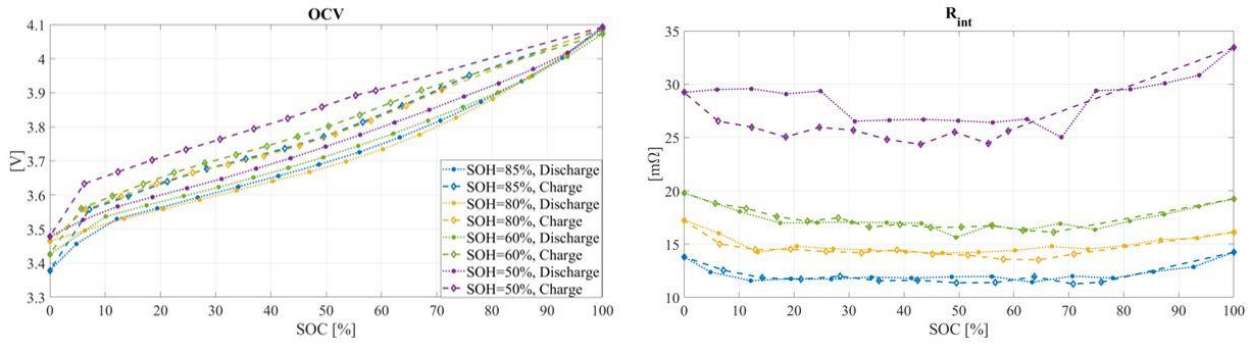

Figure 4-4: Open circuit voltage (on the left) and internal resistance (on the right) evaluation for the NMC under test at different SOC and SOH during the charging/discharging phase

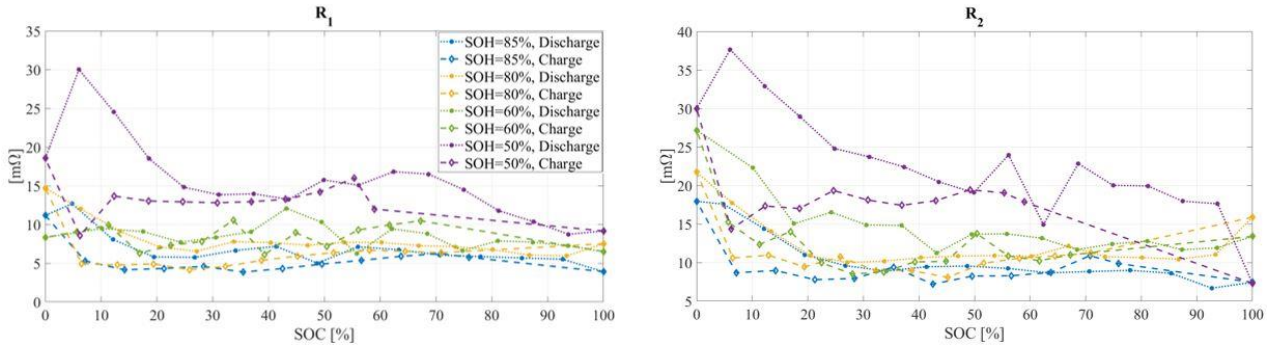

Figure 4-5: Resistances of RC-blocks evaluation for the NMC under test at different SOC and SOH during the charging/discharging phase

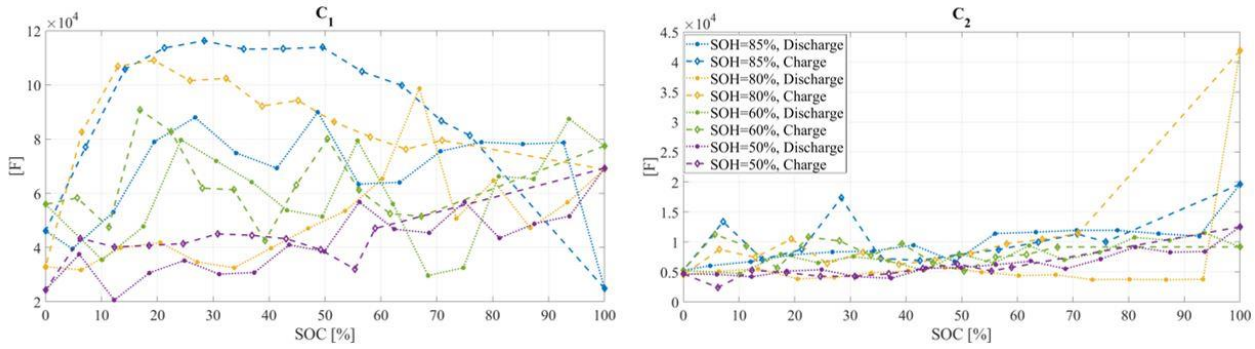

Figure 4-6: Capacitances of RC-blocks evaluation for the NMC under test at different SOC and SOH during the charging/discharging phase

4.1.5 Model validation

The voltage simulated by the battery virtual model depends on the differential equations system (Equation 4-7): this model is implemented in the Simulink simulation platform, as given in Figure 4-7. The model parameters were identified by the singles NMC cells during the characterization test. Modifying the setup parameters, the users can build the desired battery pack (nominal voltage and nominal capacity) choosing the appropriate series/parallel configuration of the NMC cells (3.7V, 20Ah). The battery model will be used in the next case study of battery second life applications, shown in chapters 5 and 6. The model validation process is carried out by comparing the measured and simulated battery voltage evolution during the current pulse test, both in discharging and charging, shown in the Figure 4-8 (test performed on the cell #4 (SOH 85%)). The absolute voltage error is defined as the difference between the experimental voltage measurements data and the simulated voltage:

$$\varepsilon_v = | V_{batt,measured} - V_{batt,simulated} |$$

Equation 4-10

An example of absolute voltage error results obtained is shown in Figure 4-9 (test performed on cell #4 (SOH 85%)). We infer by results given in Figures 4-8 and 4-9 that the battery model describes accurately the voltage evolution in the range [10,90]% of SOC (error less than 20 mV). Instead, at the extreme of the SOC window, battery non-linear behavior affects the model, hence the absolute voltage error increases during the test.

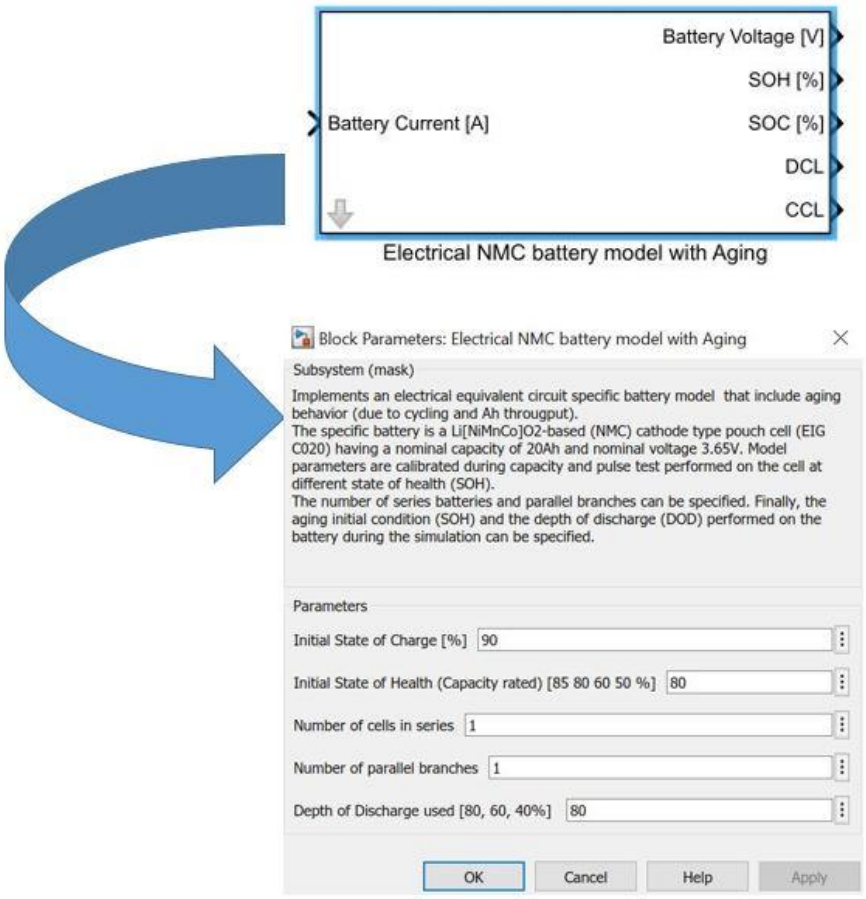

Figure 4-7: Layout of the Simulink NMC second life battery model and parameters setup

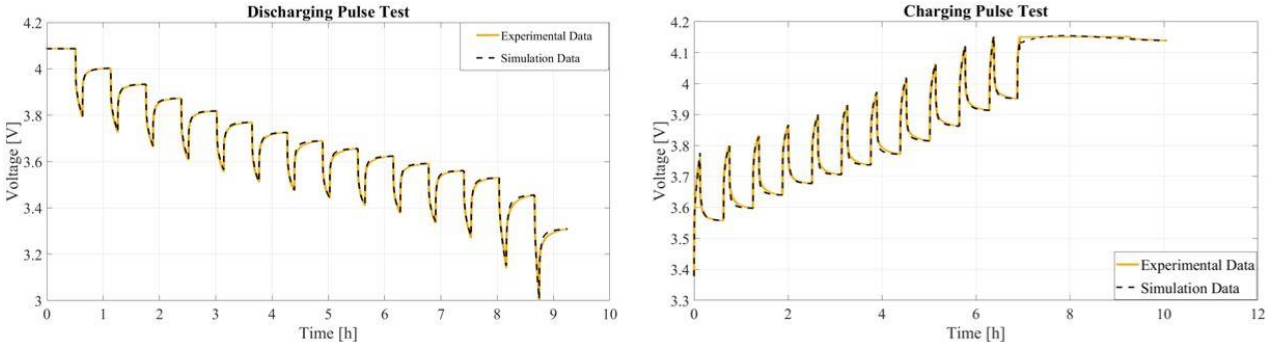

Figure 4-8: Pulse discharging and charging test: comparison between experimental and simulation voltage data

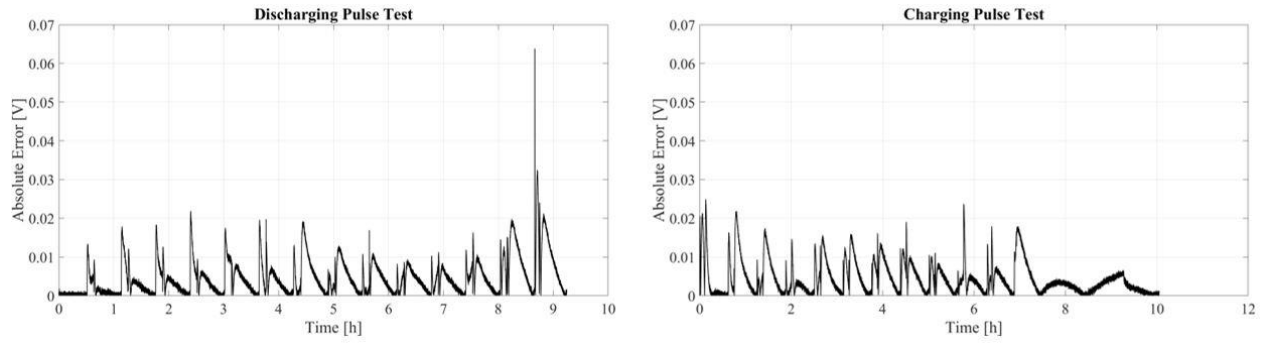

Figure 4-9: Pulse discharging and charging test: absolute error comparison between experimental and simulation voltage data

4.1.6 Aged cells models: final considerations

UNIFI has been provided a second life battery performance model which could be simply built in some simulation platforms. This model simulates the battery voltage evolution, state of charge, and state of health, giving an input current load or generator. The aging model is extracted in the ENEA research center performing eight different cycle life tests on eight NMC pouch cells of the same manufacturer. The model circuit parameters are identified in UNIFI laboratories, performing characterization tests cited in the previous OBELICS works. The second life battery model will be used in section 5 and 6, during the simulations of second life case studies.

4.2 References for second life cells model applications

[1] EIG battery official site, www.eigbattery.com
[2] Deliverable D7.2, Evaluation of international standards for lithium-ion batteries, OBELICS (2018).
[3] Deliverable D7.5, Optimization of OBELICS test procedures, OBELICS (2018).
[4] Huria, T., Ludovici, G., & Lutzemberger, G. (2014). State of charge estimation of high power lithium iron phosphate cells. Journal of Power Sources, 249, 92-102.
[5] D. Cittanti, A. Ferraris, A. Airale, S. Fiorot, S. Scavuzzo, and M. Carello, “Modeling Li-ion batteries for automotive application: A trade-off between accuracy and complexity,” International Conference of Electrical and Electronic Technologies for Automotive, Torino 15- 16 June 2017, pp.8,2017.
[6] Locorotondo, E., Cultrera, V., Pugi, L., Berzi, L., Pierini, M., Pasquali, M., Andrenacci, N., Lutzemberger, G., "Electrical lithium battery performance model for second life applications", In 2020 IEEE International Conference on Environment and Electrical Engineering and 2020 IEEE Industrial and Commercial Power Systems Europe, in press.
[7] Huria, T., Ceraolo, M., Gazzarri, J., & Jackey, R. (2012, March). High fidelity electrical model with thermal dependence for characterization and simulation of high power lithium battery cells. In 2012 IEEE International Electric Vehicle Conference (pp. 1-8). IEEE.
[8] Omar, N., Monem, M. A., Firouz, Y., Salminen, J., Smekens, J., Hegazy, O., ... & Van Mierlo, J. (2014). Lithium iron phosphate based battery–Assessment of the aging parameters and development of cycle life model. Applied Energy, 113, 1575-1585.
[9] Berecibar, M., Gandiaga, I., Villarreal, I., Omar, N., Van Mierlo, J., & Van den Bossche, P. (2016). Critical review of state of health estimation methods of Li-ion batteries for real applications. Renewable and Sustainable Energy Reviews, 56, 572-587.
[10] Saez-de-Ibarra, A., Martinez-Laserna, E., Stroe, D. I., Swierczynski, M., & Rodriguez, P. (2016). Sizing study of second life Li-ion batteries for enhancing renewable energy grid integration. IEEE Transactions on Industry Applications, 52(6), 4999-5008.
[11] Martinez-Laserna, E., Gandiaga, I., Sarasketa-Zabala, E., Badeda, J., Stroe, D. I., Swierczynski, M., & Goikoetxea, A. (2018). Battery second life: Hype, hope or reality? A critical review of the state of the art. Renewable and Sustainable Energy Reviews, 93, 701-718.
[12] Andrenacci, N., & Sglavo, V. (2017). Stato dell'arte dei modelli di invecchiamento per le celle litio-ione. Applicazione al caso di studio delle celle NMC invecchiate in ENEA.
[13] De Sutter, L., Firouz, Y., De Hoog, J., Omar, N., & Van Mierlo, J. (2019). Battery aging assessment and parametric study of lithium-ion batteries by means of a fractional differential model. Electrochimica Acta, 305, 24-36. https://doi.org/10.1016/j.electacta.2019.02.104
[14] De Sutter, L., Berckmans, G., Marinaro, M., Smekens, J., Firouz, Y., Wohlfahrt-Mehrens, M., ... & Omar, N. (2018). Comprehensive aging analysis of volumetric constrained lithium-ion pouch cells with high concentration silicon-alloy anodes. Energies, 11(11), 2948. https://doi.org/10.3390/en11112948
[15] de Hoog, J., Jaguemont, J., Nikolian, A., Van Mierlo, J., Van Den Bossche, P., & Omar, N. (2018). A combined thermo-electric resistance degradation model for nickel manganese cobalt oxide based lithium-ion cells. Applied Thermal Engineering, 135, 54-65. https://doi.org/10.1016/j.applthermaleng.2018.02.044
[16] De Hoog, J., Jaguemont, J., Abdel-Monem, M., Van Den Bossche, P., Van Mierlo, J., & Omar, N. (2018). Combining an electrothermal and impedance aging model to investigate thermal degradation caused by fast charging. Energies, 11(4), 804. https://doi.org/10.3390/en11040804

[17] Nikolian, A., Jaguemont, J., de Hoog, J., Goutam, S., Omar, N., Van Den Bossche, P., & Van Mierlo, J. (2018). Complete cell-level lithium-ion electrical ECM model for different chemistries (NMC, LFP, LTO) and temperatures (− 5° C to 45° C)–Optimized modelling techniques. International Journal of Electrical Power & Energy Systems, 98, 133-146. https://doi.org/10.1016/j.ijepes.2017.11.031

[18] de Hoog, J., Timmermans, J. M., Ioan-Stroe, D., Swierczynski, M., Jaguemont, J., Goutam, S., ... & Van Den Bossche, P. (2017). Combined cycling and calendar capacity fade modeling of a Nickel-Manganese-Cobalt Oxide Cell with real-life profile validation. Applied Energy, 200, 47-61. https://doi.org/10.1016/j.apenergy.2017.05.018

[19] Hosen, M. S., Karimi, D., Kalogiannis, T., Pirooz, A., Jaguemont, J., Berecibar, M., & Van Mierlo, J. (2020). Electro-aging model development of nickel-manganese-cobalt lithium-ion technology validated with light and heavy-duty real-life profiles. Journal of Energy Storage, 28, 101265. https://doi.org/10.1016/j.est.2020.101265

[20] Gandoman, F. H., Firouz, Y., Hosen, M. S., Kalogiannis, T., Jaguemont, J., Berecibar, M., & Van Mierlo, J. (2019, October). Reliability Assessment of NMC Li-Ion Battery for Electric Vehicles Application. In 2019 IEEE Vehicle Power and Propulsion Conference (VPPC) (pp. 1-6). IEEE. https://doi.org/10.1109/VPPC46532.2019.8952180

5 Development of a methodology to link the appropriate second life battery to applications (grid, household, renewable)

The use of lithium-based batteries in the automotive field is particularly demanding due to the need of significant installed capacity, high energy density and power-to-capacity ratio. For this reason, literature of the last decade suggested that even after being dismantled from vehicles, partially degraded battery would still be satisfactory for other "second life" uses. In parallel, the expansion of renewable energies such as photovoltaic panels both in civil and industrial energy market suggests that coupling such discontinuous generators with storage systems could improve system flexibility, while maintaining a low environmental impact.
This section provide a suggestion for a methodology applicable to system integration of second life battery systems in existing industrial, residential or energy type plants, in order to study the system as a whole and obtain those indicators related to the interaction between energy storage, industrial plant and, in case, energy production or acquisition from grid.
According to the general approach of the OBELICS project, the suitable methodology is based on the definition of a comprehensive model which includes all main actors of the system, such as:

- The energy storage system
  - Tailored model calibration based on data acquired on used cells can be applied here
- The energy consuming system
  - Case studies: railway vehicles, mobile networks stations
- The energy production system, if any
  - E.g. renewables such as wind or photovoltaic energy
- The grid, represented by a source or sink of energy which has a certain "cost"
  - A procedure to calibrate environmental and economic cost is provided.

5.1 Energy from the grid: linking environmental and economic cost

The use of energy from the grid determine greenhouse gas (GHG) emissions that are usually described in terms of average gCO_2/kWh assessed per each country. Looking at the Italian scenario (the one selected for this application, but the method can be extended to other contexts), even if the overall value is about 260 gCO2/kWh[1], it can be seen that relevant variation are possible within the same day and across various period of their, mostly due the variability of renewable sources production.
Energy economic cost is similarly variable in terms of day of the year and hourly cost; in particular, the data presented by the Italian market manager have been assumed as reference to define the energy acquisition cost ("from" grid cost, adapted in order to achieve an overall year cost of 0.17€/kWh – tax excluded, coherently with Eurostat data [2]) and the energy "to grid" value, based on historical data for the 2019 year [3]. Data are shown in Figure 5-1.

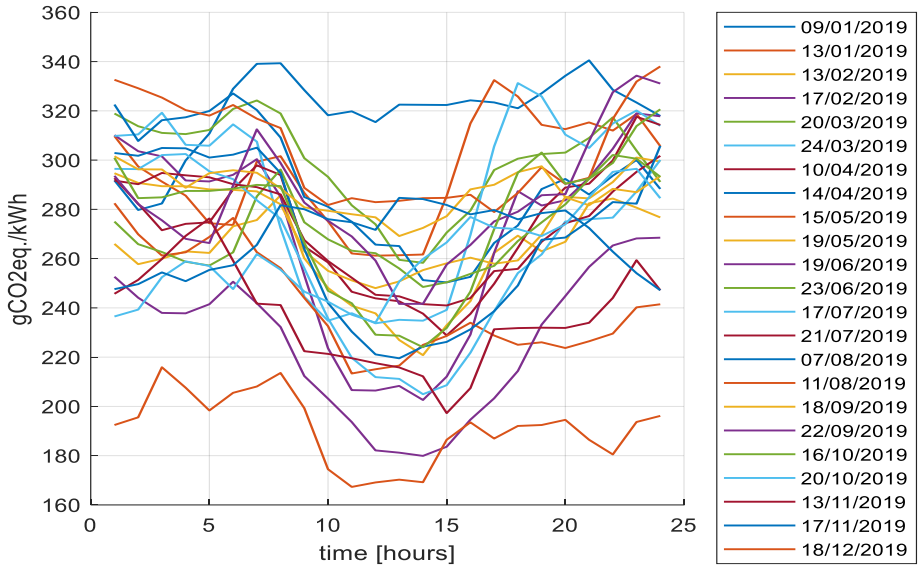

Figure 5-1: Carbon intensity variability of electric energy generation in Italy depending on day hour and year period. Data have been processed from Italian grid manager source [1]. Lines represent 24 typical days (per each of the 12 months, one weekend and one weekday value have been plot).

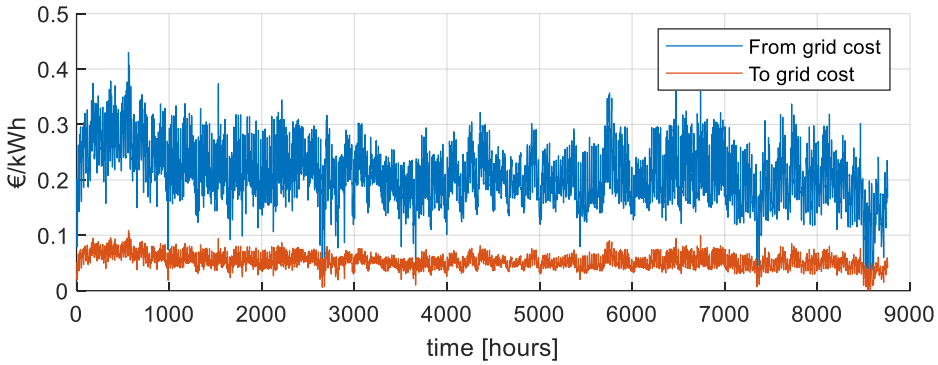

Figure 5-2: Energy cost in €/kWh per hour of the year (0-8760) on the Italian market.

For optimization scopes, an aggregated economic and environmental cost for energy acquired from grid (see Figure 5-3) has been defined according to the following definition:

$$CA = \alpha_1 \times \frac{Ce(t)}{\max\left(Ce(t)\right)} + \alpha_2 \times \frac{Es(t)}{\max\left(Es(t)\right)}$$

Where:

Ce is economic cost, normalized respect to its maximum value
Es is the environmental cost, normalized to its maximum value
α_1 and α_2 are weighting factors, set as 0.5 each for this application.

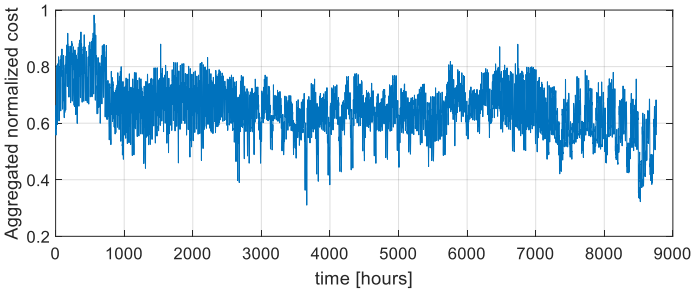

Figure 5-3: Aggregated environmental and economic normalized cost, obtained using weighting factors both equal to 0.5.

All costs have been implemented as look up tables in the model.

5.2 Chapter references

[1]. «CO2 emission intensity», European Environment Agency. https://www.eea.europa.eu/data-and-maps/daviz/co2-emission-intensity-5 (consultato apr. 15, 2020).
[2]. «Statistics Explained». https://ec.europa.eu/eurostat/statistics-explained/index.php/Main_Page (consultato apr. 15, 2020).
[3]. «GME - Gestore dei Mercati Energetici SpA». https://www.mercatoelettrico.org/it/ (consultato apr. 15, 2020).
[4]. «Home - Terna spa». https://www.terna.it/it (consultato apr. 15, 2020).

6 Definition of suitable case studies

6.1 The use of second-life battery as energy storage in tramway station: analysis, modeling, and simulation

There is wide literature information concerning the application of reversible power stations. In particular, on DC lines it's often proposed to use the application of energy storage systems based on supercapacitors [1], batteries [2] and more recently of second life storage systems [3,4] that should be made available for stationary applications by the increasing availability of used accumulators that should be available in a short-medium term scenario from the growing market of electric and hybrid vehicles.
In this work, it is proposed to perform the simulation of a tramway system with reversible substations through the usage of a hybrid symbolic modeling implemented in Matlab™.
Numerical efficiency and flexibility of proposed model is used to evaluate on a benchmark test case how reversible subsystems can contribute not only to evaluate increased efficiency levels associated with the adoption of reversible power stations, but a more flexible management of timetables with respect to foreseen system efficiency.
Optimization of tramway and metro timetables is often the result of complex optimizations in terms of reliability, energy efficiency and robustness with respect to various kind of events that could perturbate traffic on railway lines [5],[6] which are often performed with relatively simple models that must be numerically light in order to perform iterative optimizations. In this work, the authors use the proposed model to demonstrate how the usage of reversible power stations produce an advantage not only in terms of energy optimization but also in terms of effort needed for Timetable optimization, almost reducing the need of complex models to evaluate optimal scheduling of incoming trains in order to maximize regenerative braking.
According to cited work from the literature a major attention is the sensitivity of results with respect to various vehicle and line parameters, which is often neglected in literature.

6.1.1 Proposed Benchmark Test Case and Corresponding Implementation of the Model

In this work, the study of a Sirio Tramway is proposed since this is a widely diffused system which is widely known in literature and often adopted as benchmark test case for the investigation of different stationary storage solutions [7]. In particular in this work we consider the version of Sirio platform that is currently installed on Tramway lines of the city of Florence in Italy[8] to which are referred data and pictures of Table 6-1 and 6-2, and Figure 6-1.

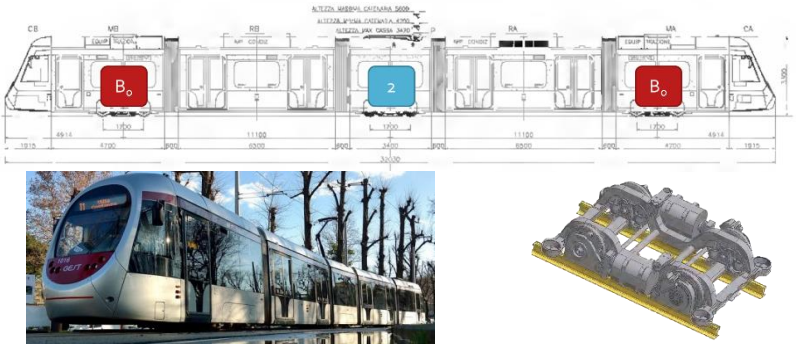

Figure 6-1: Benchmark test case Sirio-Firenze Tramway

Table 6-1. Main features of modelled Hitachi Sirio-Firenze Tramway

Parameter	Value	Parameter	Value
Max Length	32030[mm]	Max Speed	70[kmh]
Max Width	2400[mm]	Residual Acceleration	>0.1 [m/s2]

Wheel radius (mean wear)	635 [mm]	Mean Acceleration	1 [m/s2]
Height	3414 [mm]	Jerk	1.1 [m/s3]
Tare load	39.768 [t] ± 4%	Max Slope	7%
Max load	58.808 [t] ± 4%	Voltage	750 (+20%, -33%) [V]
Axle load	About 11[t]	Max Current	1200[A]
Unsprung Axle Mass	About 1.25[t]	*Data from manufacturer	

Table 6-2. Simplified Feature of Line Considered for Sirio Firenze Line

Parameter	Value	Parameter	Value
Eq. Copper Section of the Line	120[mm2]	Max and Nom. Voltage of the line	900-750 [V]

Proposed analysis requires a relatively efficient implementation in order to perform a large number of iterative simulations so authors preferred to implement a script model in Matlab™ that can be easily implemented and compiled for a fast execution with modest computational resources:

- First, a symbolic solution of equations representing the electrical behavior of the line including moving loads represented by vehicles is calculated using Matlab Symbolic Toolbox™.
- Then a kinematic mission profile of vehicles imposing kinematic (jerk, acceleration limits) and power constraints.
- Finally Symbolic Solution of the line is implemented efficiently using a function that can be automatically generated and compiled for an assigned target assuring a high computational efficiency.

6.1.2 Simplified Simulation Scenario: Simulation and Results

In Figure 6-2 it's shown the simplified scenario adopted for simulation: two trams are travelling in opposite directions between two stops describing the same kinematic profile: tram 2 starts from stop 2 with a delay *dt* respect tram 1 which is scaled respect to *T* with a scaling factor k_d.*T* is the time needed to travel to cover the distance *L* between two stops.V_i I_i and are respectively the collected voltage current collected by the i-th tram. Power collected by the i-th tram, W_i is imposed and it's coherent with tram mission profile that is calculated according imposed kinematic (jerk, acceleration and speed limits) and performance constraints (max torque and power available on the tram). An example constrained mission profile referred to a distance L of 1500 meters is visible in Figure 6-3.

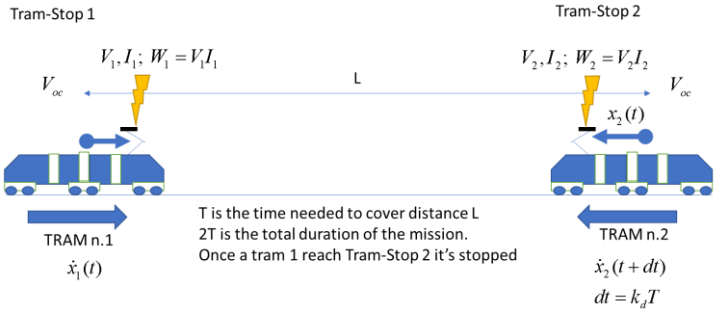

Figure 6-2: simplified scenario adopted for simulation

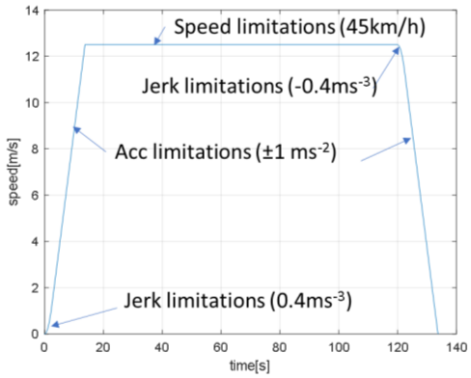

Figure 6-3: Example of constrained mission profile (max speed 45 kmh, max acc. ±1ms-2, max jerk ±0.4ms-3)

In Figure 6-4 it's shown a first example of simulation in which for a distance *L* of 1500 m (max weight of the tram is supposed) is evaluated energy consumptions for different power station layout according the value of the delay fraction k_d (k_d=*dt*/*T*): with conventional, single quadrant power station (red line in fig. 3) there is a very precise value of k_d that allows a good efficiency improvement as stated by current literature [5], [6], however with ideal reversible substation (green line in fig. 3) this optimum solution is not really recognizable; only if we suppose a reversible power station with a constant storage efficiency of 0.8 there is a negligible advantage in terms of saved energy from an optimized value of k_d . A storage efficiency of 0.8 it's supposed: typical efficiency of DC-DC converters that should be used to couple batteries to line is around 0.9-0.95; so considering a double conversion "from" and "to" batteries and some residual internal losses of cells an expected efficiency of about 0.8 is considered at least feasible.

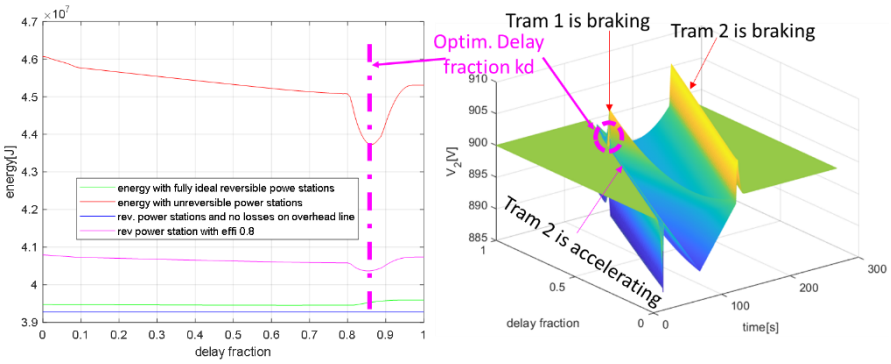

Figure 6-4: energy consumptions (left) as function of power station configurations and kd, voltage V2 collected by the second Tram as function of kd (on right)

Same Simulations have been repeated considering different distances between stops, as visible in Figure 6-4 where results are similar: with conventional power stations a relatively big energy saving (from 10 to 15%) is expected by optimizing the synchronization of the mission profile of different trams; as efficiency of applied storage system increase from a realistic value (efficiency equal to 80%) to and ideal condition an increased freedom in terms of timetables is possible. Energy consumptions of Figure 6-4 are scaled with respect to the maximum energy that should be expended without any energy regeneration for the corresponding length *L*. In this way it is possible to demonstrate that proposed storage solution is much more effective in term of energy saving for short distances between bus stops.

Finally in Figure 6-5 some further results are shown: simulations for a value of *L* equal to 500m are repeated considering different constraints in terms of maximum speed from 35 to 65 km/h without storage systems (Figure 6-6-a) needed energy has a near to monotonic behavior with respect to speed and the optimization of timetables produce an appreciable energy saving which is more appreciable for high traveling speed where higher peaks in power profiles are expected. With installed storage systems (Figure 6-6-b) it is clearly recognizable that chosen speed limit (45kmh) is clearly optimal in terms of energy consumptions, also perturbations of scheduling in terms of k_d produced limited consequences. Finally a speed of 45kmh assure a large robustness of timetables with

respect to traffic perturbations and since max speed of the vehicle is 70kmh it's relatively easy to recover delays with respect to the programmed timetable.

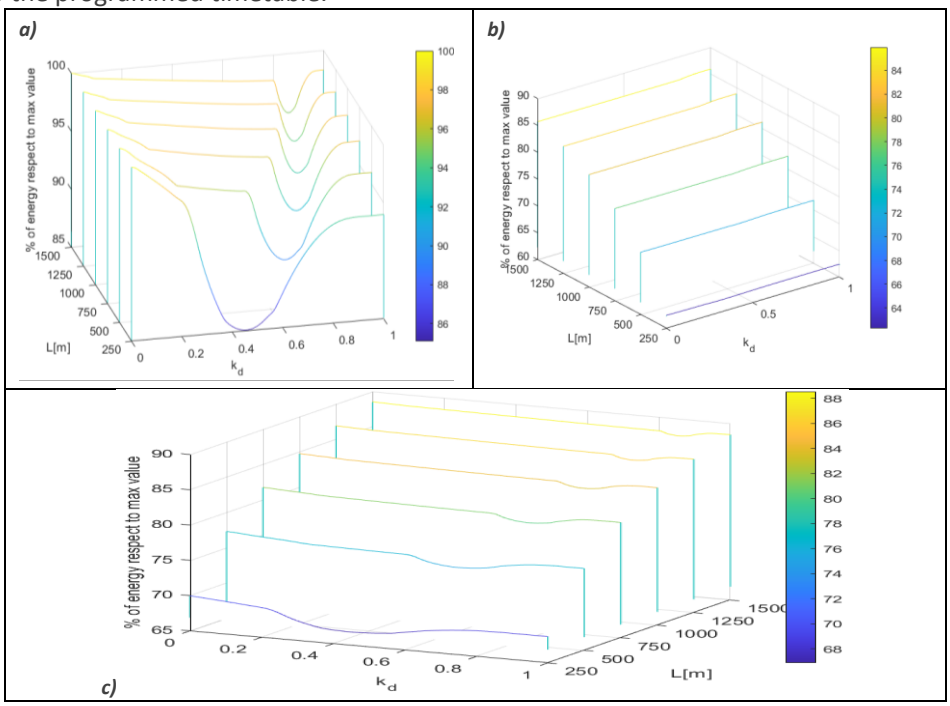

Figure 6-5: relative energy consumptions with conventional single quadrant substations (a), with ideal reversible power stations (b), with a storage that has an equivalent efficiency of 0.8, losses with different equivalent copper sections of the line

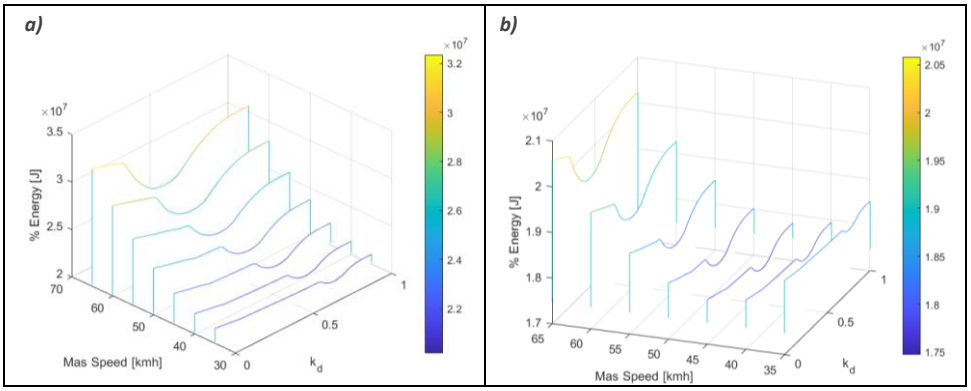

Figure 6-6: energy consumption respect to speed and kd with single quadrant powerstations (a), and with reversible power stations (b), supposed storage eff. 0.8

6.2 The use of second-life battery as energy storage in mobile network station: analysis, modeling, and simulation

The object of the study is a mobile communication station (Radio Base Cluster - RB), which is has been considered due to characteristics such as:

- The system requires energy 24 hours per day, even if the profile is variable
- Network evolution show a significant care to energy optimization and impact reduction, while performances and number of installations are constantly increasing
- the system is typically equipped with back-up systems, so that certain components (e.g. battery, inverter, chargers) would be installed anyway, even if their size and capabilities would be different
- Relevant studies on the energy profile of the systems are available.

The case study is based on the energy performance analysis of a system including a base station cluster (RB), a BESS, a PV generation unit; the system is grid-connected. Due to appropriate AC/DC and DC/DC converters, power flux is possible in a bidirectional way from and to the grid; energy produced by PV can be used directly or stored in the battery. System overview is provided in Figure 6-7.
The RB station is the heart of the system and from its power profile over 24 hours the whole system is sized as a consequence. According to literature data [9], the power consumption depends on the area of application (e.g. expressed through the area services – in km^2 – and depending on the density of users per area, see Table 6-3), which mainly determines the capability of the installation, while the hourly load is variable depending on the scenario and on the day of the week. Detailed models for power consumption will be defined in next section.

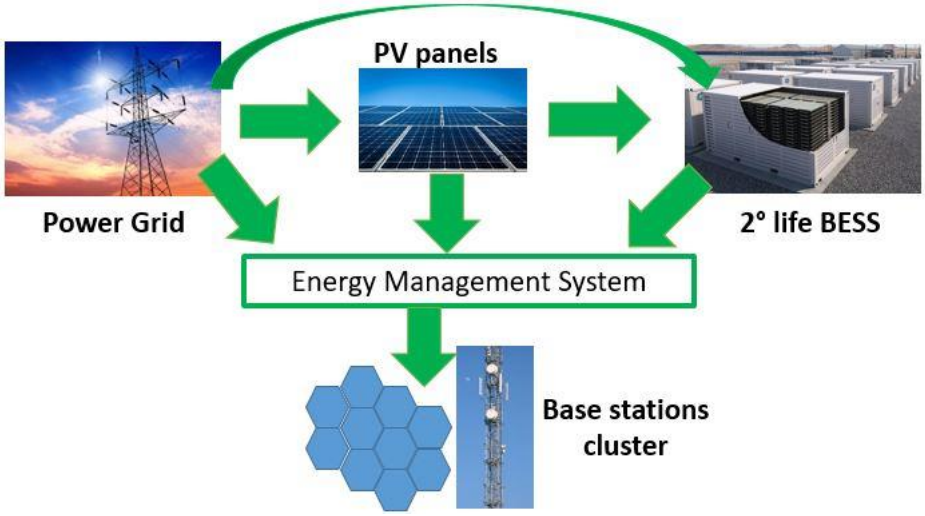

Figure 6-7: The mobile access network plant

Table 6-3. Typical traffic for various area type.

Area type	Traffic peak [Mbps/km^2]	User Density [p/km^2]
Super dense urb (SDU)	750	20000
Dense urban (DU)	110	3000
Urban (U)	40	1000
Sub urban (SU)	20	500
Rural (RU)	4	100

6.3 Energy consumption model

In the second case study, the power consumption model of a mobile network station corresponds to the electric load to which the electric energy sources must support. The model is realized according to previous research works found in the literature. In this work, the mobile network station considered is a representation of the long-term evolution (LTE) cellular network 4G standard. This network is composed of a variable number of Multi-Input and Multi-Output (MIMO) antennas micro-cell base stations (BSs) which cover the mobile traffic demand of a defined area $[km^2]$.

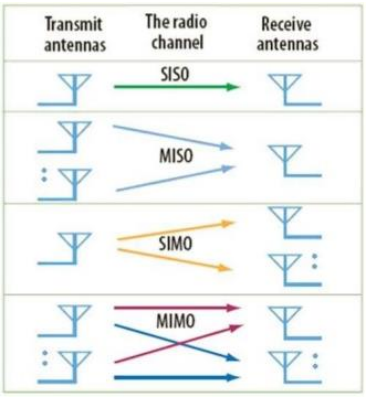

Figure 6-8: MIMO transmit antennas model [10]

The transmission model of the single MIMO micro-cell is shown in Figure 6-1. The micro-cell BS covers the traffic demand of a hexagonal area A_{BS} of radius R (≤ 1 km). Then, the number of required BSs which cover an area A can be written as:

$$N_{BS} = \frac{2A}{3\sqrt{3}R^2}$$

Equation 6-1

The power consumption of the transmit signal by the single antenna to the user is represented by the parameter P_{TX}. However, propagating the transmit signal through space, there is attenuation in power density of it. The path loss parameter P_{LOSS} assesses the value of this attenuation. The path loss model is given as follows:

$$P_{LOSS} = \frac{G\lambda^2}{L(4\pi)^2 d^{\alpha}}$$

Equation 6-2

Where G is the antenna gain, λ is the wavelength, L is the link margin, d is the transmission distance and α is the path loss exponent. The parameter values are shown in Table 6-1, referring in[11], except for the parameters d and α. Transmission distance is computed by using uniform randomization of the user's distribution in the BS's hexagonal area. The path loss exponent α depends on the type of area in which the transmit signal is propagated; this value is measured by experimental tests shown in [11], [12]. Considering a cluster of BSs which cover an area A, the total power transmit depends on the traffic demand by the user's population. In this case study, two different traffic scenarios are considered: the first is dominated by business users, the second corresponds to residential users. 24 h real traffic traces are provided by an Italian mobile operator and are depicted in Figure 6-2 for different days, with a step time of 30 mins.

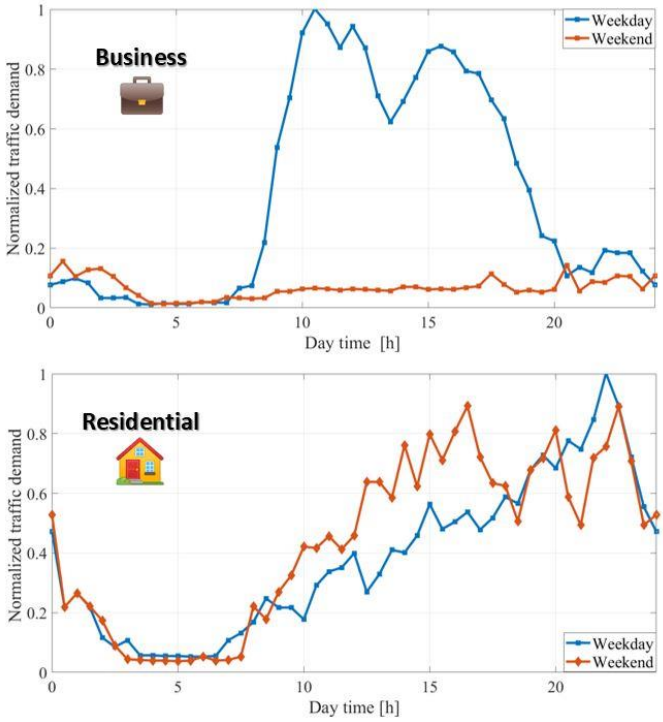

Figure 6-9: Normalized traffic per different days and use scenarios

Traffic demand is measured per area unit, hence in $Mbps/km^2$. The peak traffic demand depends on the population density of the area covered. Based on demographic data, a country can be divided into different parts, depending on the population density. A common division is to categorize a country into six main deployment areas: super-dense urban (SDU) areas (representing the metropolis), dense urban (DU), urban, suburban (SU), rural (RU) and wilderness areas (W) (typically unpopulated). The population densities and the peak traffic demands of the cited area types are shown in Table 6-2, referring to the EARTH project work , revisited in [9].

Given the traffic demand profile, the target area (type and size), corresponding to the number of BSs the number of the transmit antennas N_{TX} of the single micro-cell BS and a path loss P_{LOSS} model (Equation 6-2), we consider another important property of the cell BSs. Indeed, every BS can operate in mode ON/OFF with an energy management policy. In this work, assuming that we can predict the total network capacity (C_{net} in $Mbps$) profile of the next day, we can switch many BSs to minimize the power consumption of the mobile network.

To calculate the optimal number of ON BSs, an assumption must be done, concerning the criteria of the MIMO antenna's transmission. In every BS, the Transmit Antenna Selection (TAS) criteria are applied. When TAS is employed, we assume that only one antenna is selected from the set N_{TX} transmit antennas. The antenna selected, through feedback comes from the receiver, maximizes the signal-to-noise-ratio (SNR) transmission. In this way, BS saves power since only one radio-frequency chain remains active.

Given the last assumption, the capacity C_{net} of the total network depends on the following equation:

$$C_{net} = N_{BS} W \log_2\left(1 + \frac{N_{TX}\gamma}{1 + N_{TX}\xi^{-1}\gamma}\right)$$

Equation 6-3

Where W represents the channel bandwidth; γ represents the SNR of the BS, employing the TAS criteria [11] it is calculated by the following equation:

$$\gamma = \frac{P_{LOSS} P_{TX}}{\sigma W}$$

Equation 6-4

Where σ represents the thermal noise power spectral density per Hz. In Equation 6-3, the parameter ξ represents the SNR due to interference between antennas. In this work, we ideally assume that $\xi \to \infty$, hence, full interference cancellation.

Given the network capacity by the traffic profile, considering the Equations (6-1)–(6-4), and assuming that for every BS area covered there is the same number of mobile users, the minimum number of the ON BS yields:

$$\begin{cases} N_{BS} = \dfrac{C_{net}}{W \log_2\left(1+\dfrac{N_{TX} P_{Loss} P_{\max}}{\sigma W}\right)} \\ s.t. \\ N_{BS} > \dfrac{2A_{\text{cov}}}{3\sqrt{3}R^2} \end{cases}$$

Equation 6-5

Where P_{max} is the maximum transmit antenna power. Therefore, given the number of ON BSs, according to Equation (6-5), we can extract the required power transmitted by single BS considering the Equation (6-3)(6-4):

$$P_{TX} = \frac{\sigma W}{N_{TX} P_{LOSS}} \left(2^{\frac{C_{net}}{N_{BS} W}} - 1 \right)$$

Equation 6-6

To compute the total network power consumption we employ a model, combining the linear model used in[11], [12], considering the impact of the backhaul system [13].

$$P_{net} = N_{BS} \left(\hat{N}_{TX} \left(k P_{TX} + P_1 \right) + P_2 \right) + P_{backhaul}$$

Equation 6-7

Where $\hat{N}_{TX} = 1$ is the number of active transmit antenna, by employing the TAS criteria. The parameter k is the gain that encompasses the effects of power amplifier drain efficiency, cooling, DSP, and supply losses. The power consumption depending on the transmit antenna's circuit losses is denoted by P_1, while P_2 does not depend on the antenna's circuit. Finally, the power consumption of the backhaul system is denoted by $P_{backhaul}$. The backhaul station manages the control unit of downlink/uplink interfaces of the entire mobile network area. The layout of the backhaul considered was taken from [13] and depicted in Figure 6-3. The impact of the backhaul, in terms of power consumption, can be written as:

$$P_{backhaul} = \left(\frac{N_{BS}}{\max_{dl}} \right) P_{switch} + N_{BS} P_{dl} + N_{ul} P_{ul}$$

Equation 6-8

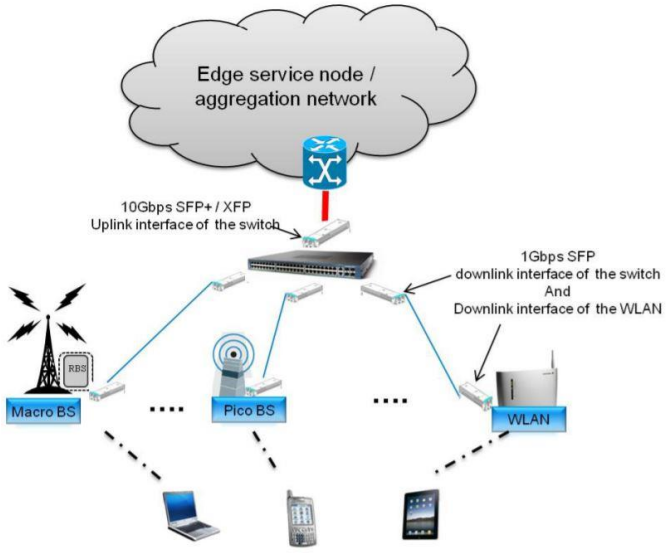

Figure 6-10: Backhauling layout considered in [13]; in this work, we consider only micro cell BSs.

The power consumed by the backhaul takes into account the power consumed by:

- Downlink interfaces P_{dl}, dedicated to each BS;
- Uplink interfaces P_{ul}, dedicated to each access switch: the number of an access switch is denoted by the variable $N_{ul} = Ag_{tot}/U_{max}$, where Ag_{tot} is the total traffic aggregated at all switches and U_{max} is the maximum rate supported by each uplink interfaces
- Power consumed by the access switch P_{switch} calculated according to [13]:

$$P_{switch} = \delta P_{switch,\max} + (1-\delta)\frac{Ag_{tot}}{Ag_{\max}} P_{switch,\max}$$

Equation 6-9

Where $\delta \in [0,1]$ is a weighting parameter, $P_{switch,max}$ is the maximum power consumed by the switch.

6.3.1 Model validation: simulation results

In this section, model accuracy is presented, by comparison with simulation results and reference results taken in previous work [11]. The mobile network power consumption model is defined according to Equation (6-1)-(6-9). The simulation parameters are shown in Tables 6-1 and 6-2.

Table 6-4: List of parameters

Parameter	Values	Units
G	10	dBi
L	10	dB
λ	0.12	m
α	[SDU:5.5; DU:4.8; U:3.5; SU:2.7; RU:2.5]	/
W	5	MHz
σ	-174	dbm
k	3.14	/
P_1	35	W

P_2	34	W
P_{max}	6.31	W
max_{dl}	24	/
P_{dl}	1	W
P_{ul}	2	W
U_{max}	10	Gbps
Ag_{max}	24	Gbps
δ	0.9	/
$P_{switch,max}$	300	W

Table 6-5: Resulting traffic peak demand for different area type for the year 2020

Area Type	Population density [citizens/km2]	Traffic demand (2020) [$\boldsymbol{Mbps/km^2}$]
Super Dense Urban	20000	750
Dense Urban	3000	110
Urban	1000	40
SubUrban	500	20
Rural	100	4

The model is implemented in the Simulink simulation platform, as given in Figure 6-4. Receiving in input the time day hour (step-time 0.5 h) and day type (weekday or weekend), the model gives as output the total power consumption of the mobile network, the number of ON base stations, and finally the area energy efficiency $[bps/(J \times km^2)]$. This last metric reflects the ratio between the overall network capacity and energy consumption:

$$AEE = \frac{C_{net}}{A \times P_{net}}$$

Equation 6-10

Before simulation is running, we can size the mobile network, setting the number of transmit antennas N_{TX}, the area covered by single micro-cell BS R, the total area A, and the area type covered by the BS clusters, the traffic use scenario (Business or residential). The model validation consists of a reply to the same power consumption of the model used in the past works. In Figure 6-5, the day time power consumption profile is depicted in an Urban area [1000 citizens/km2], considering a Business traffic scenario: results are similar. Results are similar respect to previous work illustrated in [9]. Finally, the area efficiencies obtained in the simulations varying the number of transmit antennas and covered areas are given in Figure 6-6, which results are according to previous work carried out in [11].

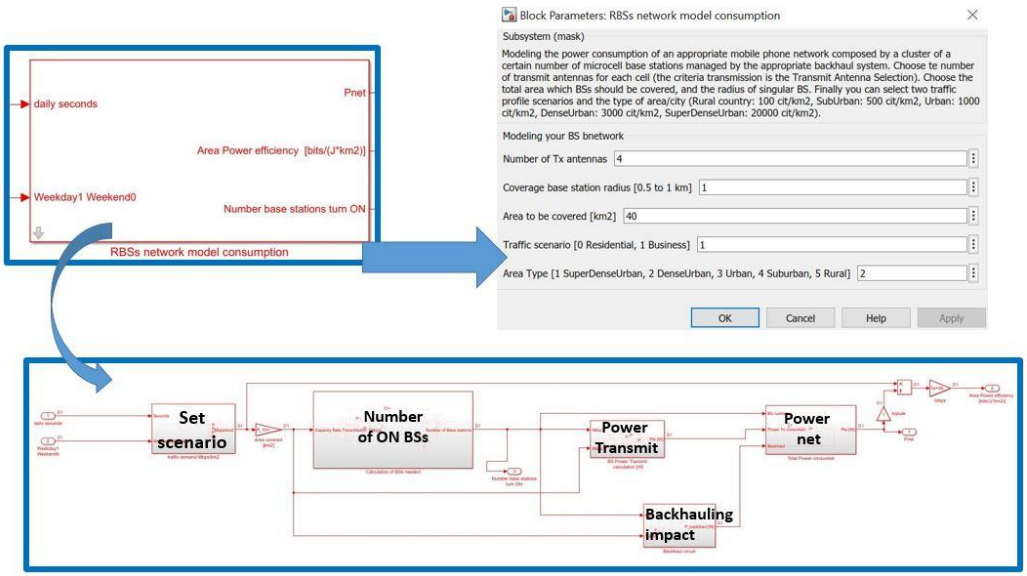

Figure 6-11: Layout of the Simulink mobile network power consumption model and parameters setup

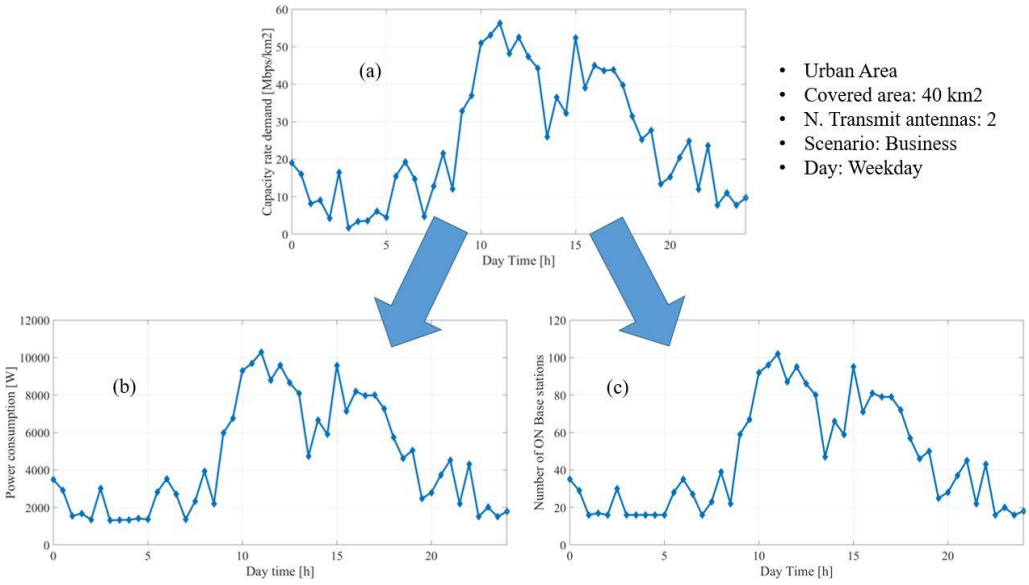

Figure 6-12: Day profile model of mobile network in an Urban area of 40 km2: (a) Traffic demand (b) Power net consumption (c) Number of ON base stations

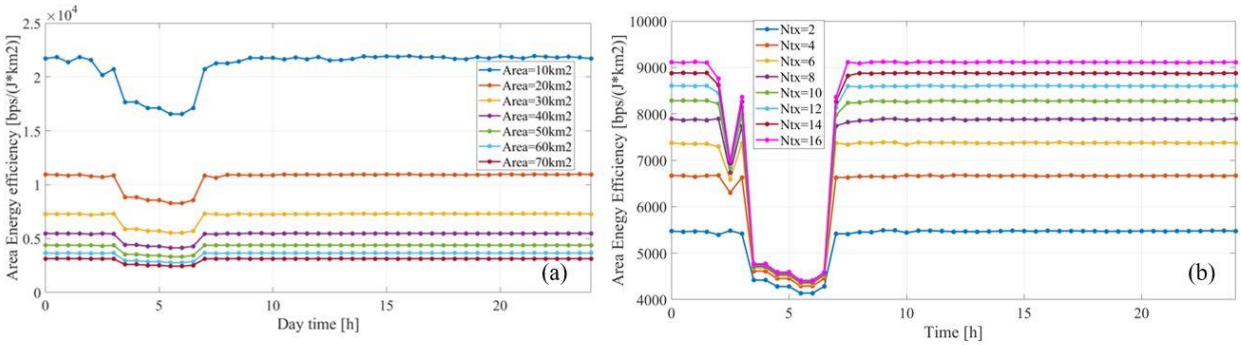

Figure 6-13: Business scenario, Dense Urban area: AEE as a function of (a) covered area ($N_{TX} = 2$) and of (b) number of transmit antennas ($A = 40\ km^2$)

In conclusion, we provide a realistic and feasible model of a mobile network composed of switching ON/OFF micro-cell BSs. This model will be used as the load time profile in the second use case study, concerning battery second life.

6.4 Energy generation model

The energy generation is provided by a PV system which, as known, provides an hourly variable power which is a fraction of the nominal peak power of the installed panels. Adopting the MERRA model as described in literature [14], PV power (normalized to peak power) is an accordance with the data shown in Figure 6-14; on a yearly bases, the average capacity factor is about 0.14, which means that a single kWp installed can produce about 1200 kWh per year overall.

Two different models have been implemented. The first one uses 4 look-up tables (one per each season) using MERRA model; model is simplified but it can be used for simplified balance simulation. The second one is based on a literature proposed model [15] integrated with other sources [16]–[18] in order to represent not only the seasonal daily average power but also the short-time variations related to external temperature and meteorological conditions, represented by proper distribution and random value generation.

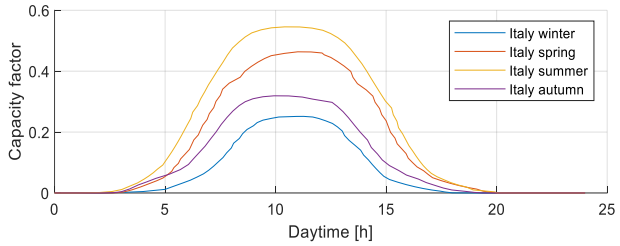

Figure 6-14: PV capacity factor variation over season and hour.

After defining capacity factor, PV power is simply obtained by scaling for its nominal peak power. On a seasonal balance, results are fully comparable to the simplified model; but per single day or per single hour of simulation, values can differ significantly. Such variability is needed to simulate system energy management reaction.
According to GaBI software [19] estimation for PV energy generation in Italy, the environmental impact has been taken into account in the final balance using a value of 64 gCO2/kWh; such aggregated value is referred to Italy production considering typical installation data and durability.

6.5 Energy management strategy

Assuming a layout similar to one proposed on Figure 6-15, adopting bidirectional AC/DC converters connected to grid and using a DC-bus with all the units interfaced on that, it is possible to achieve the hardware flexibility able to force power from and to battery on demand in any moment. This capability is necessary for the implementation of the energy strategy here defined. Overall aim is to reduce as much as possible the energy exchange with grid, so that the battery is used to store the PV energy which is not immediately consumed and to support consumption when PV power is insufficient. The strategy is implemented as follows:
At the beginning of day *n* (hour 0) the systems estimates E_grid(n), which is the difference between the expected energy consumption E_req(n) from RB system, and E_PV(n), the estimation of the energy which is going to be produced by PV using available metereological and historical data. If battery SOC was not maximum at the end of day (n-1), additional energy to restore maximum SOC is calculated.
A schedule for E_grid(n) exchange with grid is planned adopting these criteria:
If E_grid(n) is positive, energy is acquired from the system giving priority to those hours in which the aggregated cost is lower of daily average. If E_grid(n) is negative, no schedule is provided and energy is sent to the grid only when battery SOC is at the maximum admitted level.
Battery charge current limit is not exceeded during grid power acquisition
During day n simulation, the energy exchange from grid is subjected to the constraints of respecting battery minimum and maximum admitted SOC. Constraints are needed to take into account differences with pre-calculated E_grid(n) due to random variation implemented in PV and Telecommunication submodels.

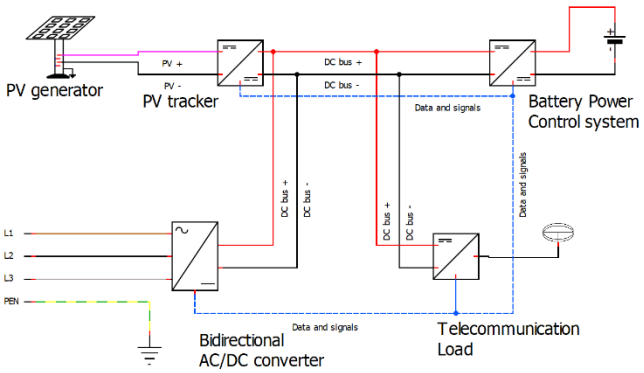

Figure 6-15: System structure layout. All peripherals share the DC-bus connection. All data are acquired by a power control unit which commands zero/positive/negative DC current from bidirectional AC/DC converter.

6.6 Full Model definition

After defining the submodel characteristics, final model has been implemented in Matlab-Simulink environment for execution (see Figure 6-16).

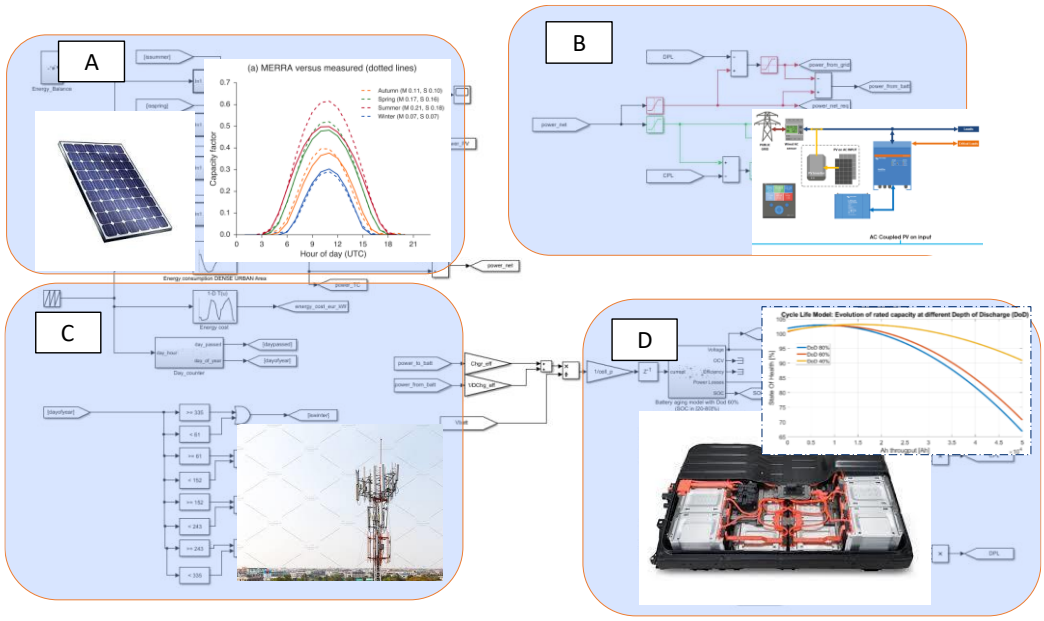

Figure 6-16: Layout of Matlab/Simulink model, including main subsystems such as: A) PV generation unit; B) Energy management and conversion unit; C) RB unit and energy consumption estimation; D) Battery derived from automotive case study, including efficiency, SOC and SOH assessment.

The sizing of the whole plant has been done starting from RB sand calculating all the other elements accordingly. Full parameters are listed in Table 6-6, and in particular:

- RB daily consumption is about 60kWh per day
- Consequently, battery has been dimensioned (according to its starting SOH) assuming that a comparable usable energy should have been stored
- Battery minimum SOC is calculated in order to guarantee at least 3 backup hours, so that it is 20%
- PV system has been assumed to be able to satisfy total energy consumption on favourable season.

As a consequence for these choices, considerable amount of energy per day are requested during winter and autumn season, while during summer and spring balance is close to zero – or even negative, so that part of the energy will be sent to grid.

Table 6-6: Parameters adopted for model sizing.

System	Parameter	Value	Unit
Battery	Min SOC	20	%
	Max SOC	80	%
	Cells in parallel	36	
	Cells in series	27	
	Nominal energy at beginning SOH	72	kWh
	Usable energy at beginning SOH	60	kWh
	Charge power limit	15	kW
	Discharge power limit	30	kW
RB system	Installed antennas	4	
	Area to be covered	10	km^2
	Traffic scenario	Residential	
	Area type	Dense Urban	
	Random variability admitted	+-25%	kWh
	Estimated energy needed (typical week day)	63.0	kWh
	Estimated energy needed (typical weekend day)	55.6	kWh
Grid	Converter efficiency	95%	
	Maximum power admitted	10	kW
PV	Nominal power (considering tracker efficiency)	13	kWp

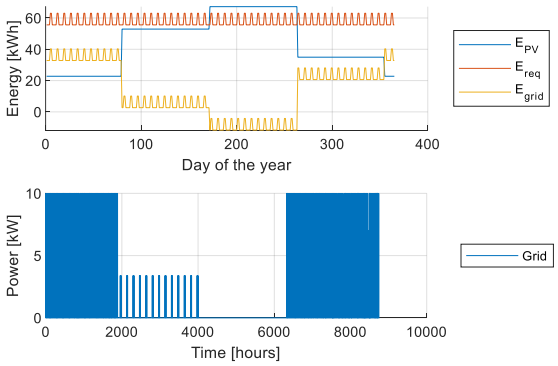

Figure 6-17: Expected energy balance (upper figure) and scheduled power requested from grid.

Operating cost results – i.e., not including plant installation -are shown in Fig. 16 and Fig. 17; they are originated by the simulation of 1 year of use also considering random oscillations of production and consumption. Three scenario are compared: a) only RB b) RB with PV production c) RB with PV and battery energy storage.

Model demonstrates that the adoption of energy storage for optimal "peak shaving" shows significant advantages if compared to solutions with PV. GHG impact is reduced up to -60% in comparison with RB alone and -50% in comparison with systems with PV and without energy storage. From an economic point of view, the operative cost is reduced significantly – up to -80% - if compared with RB alone and up to -60% if compared with systems with PV and without energy storage.

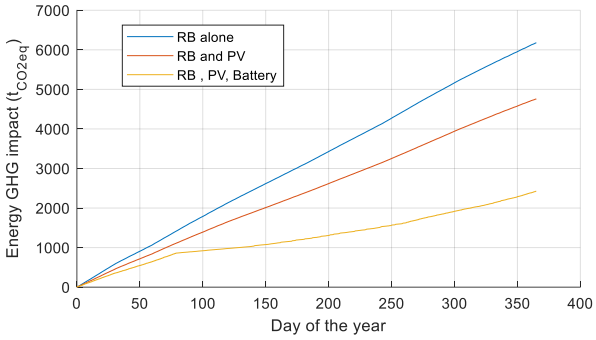

Figure 6-18: GHG emissions for RB case study, with PV, with PV and battery.

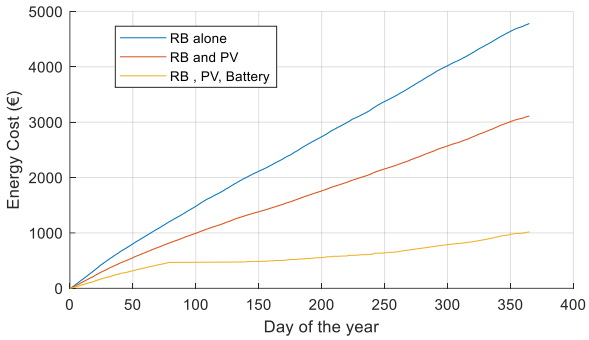

Figure 6-19: Energy cost for RB case study, with PV, with PV and battery.

6.7 Conclusions on the case study

The model here presented is able to process an energy scenario for a Radio Base system for network communication coordinating different sources such as environmental impact estimation database, network communication and energy consumption model, energy storage performance and ageing model. According to literature and primary data, all the subsystems have been modelled and calibrated in a single Matlab-Simulink environment, in order to study interactions between systems also considering randomized data. Adopting a simplified strategy for energy peak power shaving and shifting, the model shows that a large potential for impact and cost reduction – at least for the use phase – is possible due to reduced and optimized energy acquisition from grid. The peculiarity of the proposed approach is that the cost to be minimized is a combination of economic and environmental cost, which are both defined with an high level of detail. The adoption of hourly varying GHG impact, in particular, enables optimization strategies. The use of second life batteries, whose characterization and modeling is described in the present document, is possible due to the possibility to maintain peak power under acceptable limits.

6.8 References for the case study

[1] R. Barrero, X. Tackoen, e J. van Mierlo, «Stationary or onboard energy storage systems for energy consumption reduction in a metro network»:, *Proceedings of the Institution of Mechanical Engineers, Part F: Journal of Rail and Rapid Transit*, apr. 2010, doi: 10.1243/09544097JRRT322.

[2] M. Ceraolo, G. Lutzemberger, A. Frilli, e L. Pugi, «Regenerative braking in high speed railway applications: Analysis by different simulation tools», in *2016 IEEE 16th International Conference on Environment and Electrical Engineering (EEEIC)*, giu. 2016, pagg. 1–5, doi: 10.1109/EEEIC.2016.7555474.

[3] E. Locorotondo *et al.*, «Electrical lithium battery performance model for second life applications», Madrid, 2020.

[4] E. Locorotondo *et al.*, «Impedance spectroscopy characterization of lithium batteries with different ages in second life application», in *2020 IEEE International Conference on Environment and Electrical Engineering and 2020 IEEE Industrial and Commercial Power Systems Europe (EEEIC / I CPS Europe)*, giu. 2020, pagg. 1–6, doi: 10.1109/EEEIC/ICPSEurope49358.2020.9160616.

[5] X. Yang, J. Wu, H. Sun, Z. Gao, H. Yin, e Y. Qu, «Performance improvement of energy consumption, passenger time and robustness in metro systems: A multi-objective timetable optimization approach», *Computers & Industrial Engineering*, vol. 137, pag. 106076, nov. 2019, doi: 10.1016/j.cie.2019.106076.
[6] S. Su, X. Li, T. Tang, e Z. Gao, «A Subway Train Timetable Optimization Approach Based on Energy-Efficient Operation Strategy», *IEEE Transactions on Intelligent Transportation Systems*, vol. 14, n. 2, pagg. 883–893, giu. 2013, doi: 10.1109/TITS.2013.2244885.
[7] M. Guerrieri, «Catenary-Free Tramway Systems: Functional and Cost–Benefit Analysis for a Metropolitan Area», *Urban Rail Transit*, vol. 5, n. 4, pagg. 289–309, dic. 2019, doi: 10.1007/s40864-019-00118-y.
[8] L. Pugi, F. Grasso, e G. Rossi, «Energy Simulation of Tramway Systems, Simplified and Efficient Models», in *2018 IEEE International Conference on Environment and Electrical Engineering and 2018 IEEE Industrial and Commercial Power Systems Europe (EEEIC / I CPS Europe)*, giu. 2018, pagg. 1–6, doi: 10.1109/EEEIC.2018.8494431.
[9] M. Olsson, S. Tombaz, I. Gódor, e P. Frenger, «Energy performance evaluation revisited: Methodology, models and results», in *2016 IEEE 12th International Conference on Wireless and Mobile Computing, Networking and Communications (WiMob)*, ott. 2016, pagg. 1–7, doi: 10.1109/WiMOB.2016.7763182.
[10] A. Goldsmith, *Wireless Communications*. Cambridge University Press, 2005.
[11] R. Krauss, G. Brante, O. K. Rayel, R. D. Souza, O. Onireti, e M. A. Imran, «Energy Efficiency of Multiple Antenna Cellular Networks Considering a Realistic Power Consumption Model», *IEEE Transactions on Green Communications and Networking*, vol. 3, n. 1, pagg. 1–10, mar. 2019, doi: 10.1109/TGCN.2018.2868505.
[12] D. Renga, H. Al Haj Hassan, M. Meo, e L. Nuaymi, «Energy Management and Base Station On/Off Switching in Green Mobile Networks for Offering Ancillary Services», *IEEE Transactions on Green Communications and Networking*, vol. 2, n. 3, pagg. 868–880, set. 2018, doi: 10.1109/TGCN.2018.2821097.
[13] S. Tombaz, P. Monti, K. Wang, A. Vastberg, M. Forzati, e J. Zander, «Impact of Backhauling Power Consumption on the Deployment of Heterogeneous Mobile Networks», in *2011 IEEE Global Telecommunications Conference - GLOBECOM 2011*, dic. 2011, pagg. 1–5, doi: 10.1109/GLOCOM.2011.6133999.
[14] S. Pfenninger e I. Staffell, «Long-term patterns of European PV output using 30 years of validated hourly reanalysis and satellite data», *Energy*, vol. 114, pagg. 1251–1265, nov. 2016, doi: 10.1016/j.energy.2016.08.060.
[15] S. D. Cristofalo, «ProgettoCNR Energy+: metodo di calcolo semplificato per la scomposizione della radiazione solare globale e la stima della produzione da fotovoltaico.», IAMC-CNR, Palermo, 2016.
[16] T. Huld, R. Gottschalg, H. G. Beyer, e M. Topič, «Mapping the performance of PV modules, effects of module type and data averaging», *Solar Energy*, vol. 84, n. 2, pagg. 324–338, feb. 2010, doi: 10.1016/j.solener.2009.12.002.
[17] B. Ridley, J. Boland, e P. Lauret, «Modelling of diffuse solar fraction with multiple predictors», *Renewable Energy*, vol. 35, n. 2, pagg. 478–483, feb. 2010, doi: 10.1016/j.renene.2009.07.018.
[18] E. Skoplaki e J. A. Palyvos, «Operating temperature of photovoltaic modules: A survey of pertinent correlations», *Renewable Energy*, vol. 34, n. 1, pagg. 23–29, gen. 2009, doi: 10.1016/j.renene.2008.04.009.
[19] Thinkstep, «Life Cycle Assessment (LCA) Software | thinkstep», 2019. https://www.thinkstep.com/software/gabi-software (consultato set. 30, 2019).

7 Identification of possible scenarios for battery technology evolution

In the light of the need for efficient battery diagnostics, self-diagnostics and integration in other power systems, the present section is focused on such needs: communication and SOH evaluation.

7.1 Characteristics of Battery Management Systems for system integration

Generally speaking, any li-ion based battery system is equipped with control and measurement hardware which are supposed to provide a variety of functions. In this paragraph, we will use the term “Battery Management System” (BMS) to indicate the unit providing the service.
In simple systems, BMS comprehends a single unit (or board), with more functions localized on the same hardware. Depending on the integration level, on modularity and on manufacturer’s need functions can be localized on different hardware. Typical functions include:

- Cell monitoring and measurements
    - Temperature (usually, 1 sensor per module at least)
    - Voltage
    - Current (at least of total batteries)
- Cell data internal processing, to provide data such as:
    - SOC assessment
    - SOH assessment
    - Internal resistance assessment
- Battery safety
    - Connection/disconnection management (contactors control or even pyrotechnic disconnectors control)
    - Insulation quality measurement respect to battery/vehicle frame monitoring and communication
- Thermal management
    - Cooling/heating strategy application depending on available hardware (e.g. coolant pump; coolant fan; Peltier Cells contro etc.)
- Battery self-maintenance
    - Cell balancing hardware and software to compensate possible voltage and charge unbalance, usually generated by different self-discharging ratio
- Battery data and availability communication
    - CANbus communication (eventually redundant)
    - Additional analog signals communication (ON/OFF digital and analog pins).
- Special test/measurement execution: mostly present at research/experimental level
    - Hardware for internal temperature assessment
    - Hardware for on-board impedance spectroscopy execution

Most vehicles are equipped with devices providing at least features such as monitoring, communication, balancing, safety (through connection/disconnection of mechanical or solid state contactors) and to integrate them successfully into other systems at least correct communication is necessary. Vehicle communications, however, are often kept reserved due to confidentiality but also safety reasons (e.g. impede hacking, modifications and tampering of devices).

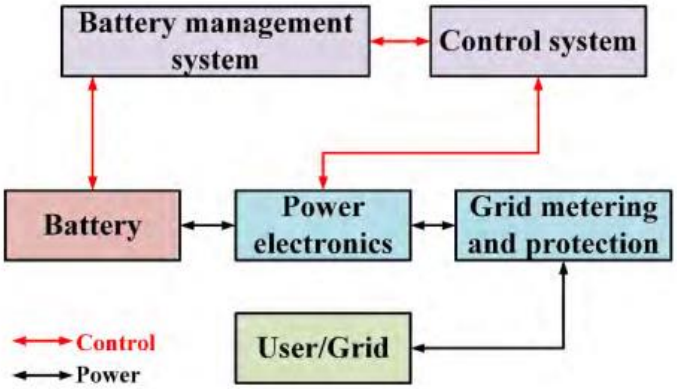

Figure 7-1: typical use of battery system according to [1]. BMS is communicating with other control systems installed in the destination plant.

In case that battery systems are going to be reused, the following capabilities should be considered:

- In case of repurposing through full remanufacturing, modular pack rebuilding is possible, so that BMS is probably going to be substituted. In this latter case, the existing BMS should be able to communicate "historical" values of the battery group (Ah throughput, estimated SOH; average C-rate etc.). An example of minimal set of data to be communicated to assess battery SOH during repurposing is shown in Table 7-1.
- In case of repurposing through direct module/pack reuse, BMS is expected to be reused directly. In this case, BMS should be able to communicate with the new system using a suitable standard and interpreter.
    - The minimum signals to be exchanged is described in Table 7-2, which is a subset of the "model identity card" defined in early OBELICS phases; without the availability of such data, battery systems cannot be used in a safe and organized manner.
    - It is necessary that BMS and destination plant can communicate directly (e.g. through CANbus) or with the interposition of a "gateway" between the two.

The design of a proper communication gateway, usually applied in early or research applications (see [2]), requires the knowledge of communication standard from the BMS; in case of CANbus signals, it essentially consists on a list of pre-determined frames of data communicated at a regular interval (usually 8 bytes per each identificatory) or in a table of information exchanged under request. Even if frame communication protocols are usually defined by suitable standards – a frequently used one in automotive applications is SAE J1939, physical layer being defined by ISO 11898 series – the frame characteristics per each data identificator and the handshaking protocols for release-under-request information are usually confidential and can differ between manufacturers, thus hindering the possibility of battery portability from vehicle to other systems.

Table 7-1: Historical data to be stored on the BMS for repurposing diagnostics

Parameter	Unit	Estimation method
Battery total throughput	Number of cycles Or Ah	Kept in memory during service
Battery total life	Hours or days or years	Kept in memory during service since first start-up
Estimated SOH	% on nominal capacity Or % on reference impedance	Estimated during battery service self-data processing

Detailed SOH (if any dedicated hardware exist)	% on reference impedance Or Actual cell impedance	Estimated through dedicated on-board hardware (e.g. impedance spectroscopy module)
C-rate history	Time spent on a certain C-rate (vector of data)	Estimated during battery service self-data processing
Temperature history	Time spent at a certain temperature (vector of data)	Estimated during battery service self-data processing
Combined temperature and C-rate history	Time spent at a certain temperature and C-rate (matrix of data)	Estimated during battery service self-data processing

Table 7-2: Data to be exchanged between BMS and plant during in-life service: proposal of a minimal set.

Parameter	Unit	Estimation method
Battery current	A	Sensor
Battery maximum power (discharge)	W	Internal algorithm
Battery maximum power (charge)	W	Internal algorithm
Battery coolant temperature	°C	Sensor
Battery SOC	%	Sensor data processing
Battery SOH	%	Sensor data processing
Battery temperature	°C	Sensor
Battery availability	Boolean	Internal algorithm for self assessment (failures of BMS/Cells)

7.1.1 Standard communication approach based on CANopen data

As a proposal for battery portability, the adoption of a shared standard between different vehicle manufacturers should be promoted among manufacturers in order to enable the possibility of economic installation on second life applications regardless of the origin of the battery. The requirements for such solutions should be:

- As a physical layer, the CANbus line should be galvanically separated to the high voltage part of the battery to guarantee safety during use
- The communication of the minimum set of parameters needed for battery reuse (see Table 7-2) should be done on separate data frame from those adopted during first life and should be in read-only state, in order to reduce the risk of vehicle hacking.
- Communication data, to be compatible to most existing standards (SAE J1939 being particularly relevant) should be done at 250 kbps
- Communication protocol should be similar to the one adopted by a large number of industrial devices, such as PLC, converters, chargers, motor drivers and similar
    - The CANopen standard is a suitable candidate due to its worldwide diffusion and it has been already proposed in literature for battery applications [3].

In particular, CANopen communication is based on four different communication sets which provide suitable characteristics, such as:

1. Safety: It is based on the continuous data exchange between devices. Each one is supposed to manifest himself on the shared network using and “heartbeat” signal, communicating the state (e.g. stopped, pre operational, operational). Network Management protocol (NMT) ensures that operation can start if all devices are providing correct heartbeat and one master is eventually setting the other to “operational” status; in absence of such signals, timeout principles ensures self-shutdown of the devices interacting with each other.
2. Simple communication, monodirectional (from battery to system): for the scope Process Data Objects, (PDO), can be used: it is a type of message with a variable content which can be published under request or continuously, thus providing data to the system in a reproducible manner
    a. Timeout-based shutdown solutions can also be implemented on the basis of correct PDO reception by the system, thus ensuring that battery is used only if BMS is efficient and all measurements are known.
3. Advanced communication, eventually reserved for the manufacturer, bidirectional (from battery to system and vice versa, in read or write mode); for this scope, Service Data Object (SDO) can be used: it is a protocol which can be adopted to request data, change settings, modify PDO content, read/write flags on the system.

7.2 State of health (SOH) diagnosis based on impedance spectroscopy

The following paragraph introduces SOH estimation using a reduces hardware set in order to define the potentiality of such diagnostics methodologies in various levels of battery life, such as:

- During repurposing phase, single battery parts (cell, modules) can be tested with onboard systems in other to assess the effective SOH of the system not only on the basis of its history but also depending on its measured impedance.
- During in-service phases (e.g. as second life storage), the periodic execution of SOH assessments through on board devices can be adopted for prognostics, so that degradation can be monitored frequently and if an acceleration in ageing is advised corrective strategies can be adopted (from battery power reduction to planned substitution of cells/modules/pack). This approach can help in reducing the risk of unplanned system failures.

7.2.1 Brief Description

The aging behavior of lithium batteries has a profound impact on their performance in terms of energy, power efficiency, and capacity stored, as demonstrated in sections 4.1 and 4.2. The battery is in end-of-life (EOL) in the automotive field when the rated capacity is at 85-80% of nominal capacity. Especially for EOL batteries, so ready for possible second use, there is an increasing need to continuously monitor their performance and SOH. Despite many research work are focused on monitoring battery state, the SOH is the weak point of the current research. Moreover, the aging phenomena after the EOL are not known. In this section, we investigate the aging phenomena of EOL automotive batteries through electrochemical impedance spectroscopy EIS. By experimental EIS tests, there are many ways to correlate battery SOH and EIS, especially when the battery is in second use.

7.2.2 State of the art of SOH monitoring methods

Despite the importance of battery SOH analysis, it still does not a consensus in the literature on how the SOH should be determined. Battery SOH is a metric to evaluate the aging level of batteries, which often includes capacity fade and/or power fade [1]. Hence, monitoring battery capacity degradation or changes of internal impedance defined in a wide frequency band, we can denote battery SOH.

In the last decades, several mathematical methods for SOH estimation are proposed in the literature. There are three different approaches.

- **Model-Based observers:** the model-based method can provide the internal resistance or battery capacity, by fitting voltage or current, employing an appropriate analytical model and several algorithms, such as

least square filters [5], Kalman filters [6], sliding mode observers [7], etc. However, they show a drastic trade-off between model accuracy and computational efforts.

- **Data-Driven Methods:** these models don't rely on the definition of a battery model to estimate battery aging. However, is difficult to obtain an effective training set.
- **EIS:** Performing a frequency response analysis of the battery, several internal degradation processes of the battery can be monitored [8]. However, direct measurements of battery impedance are affected by temperature and SOC variations.

In this section, the EIS test is performed on different aged batteries at six various SOC, considering a fixed temperature of 25°C.

7.2.3 Battery electrochemical impedance spectroscopy (EIS)

Exciting the battery in current, by using a periodic signal or a signal realization of a stochastic dynamic process [9], and observing the voltage response, we can identify the battery impedance in a frequency band. Because we execute a frequency analysis, the battery system must be considered as a linear and time-invariant dynamic system. Hence the EIS test will be performed with less energy consumption (no SOC variations) and no variations of external/internal factors such as temperature. Usually, EIS results are presented in the Nyquist diagram, comparing real impedance values with the negative of the imaginary impedance values, because batteries showed ohmic-capacitive features in the major part of the interested frequency range. Figure 7-1 shows the general shape of battery impedance in the Nyquist diagram.

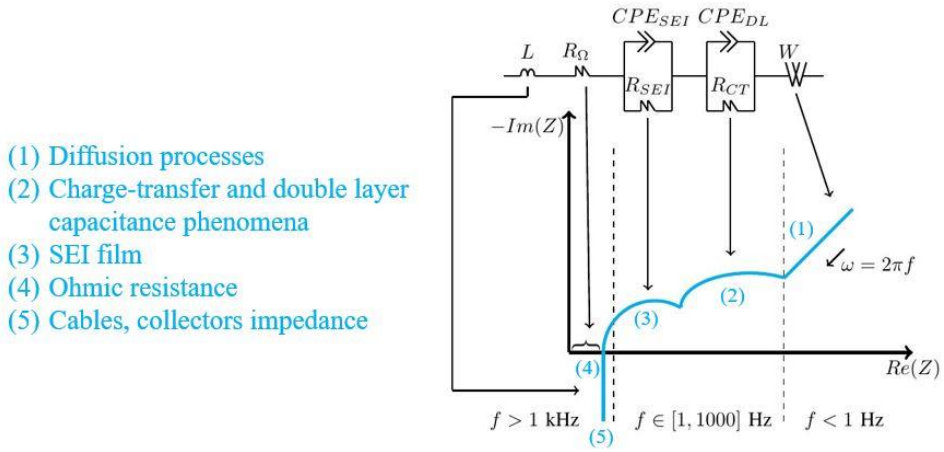

Figure 7-2: Reference spectrum of lithium battery in a wide frequency range and battery EIS modeling.

Generally, the battery impedance curve can be divided into five well-separated frequency band sections, which describe different internal processes. Starting from low frequency and arriving at high frequency, it is possible to observe:

- **Diffusion processes:** diffusion of lithium particles in active material of the electrodes at very low frequency.
- **Charge-transfer and double layer capacitance phenomena:** transfer of lithium particles between electrolyte and electrodes are represented by using charge-transfer resistance and double-layer capacitance phenomena.
- **SEI film:** the solid electrolyte interphase film is created in the electrolyte/anode interface during the first cycles of the battery.
- **Ohmic resistance:** The current delivered/supplied by the battery comes with voltage drop due to collectors, active material, electrolyte, and separator, represented by static resistance found at zero-crossing frequency.
- **Cables, collectors impedance:** inductive behavior of the battery, due to the reactance of battery cables and collectors, at the highest frequency.

We can identify an equivalent circuit impedance model by fitting experimental data. Randles circuit model configurations are more diffused in the EIS field [10]. In this section, the model considered is shown in Figure 7-1, in which, different circuit parameters model different battery internal processes. Starting from the highest frequency band, cables and collectors impedance are modeled by the inductance parameter L; Ohmic resistance is modeled by the resistance parameter R_{Ω}. SEI film, charge-transfer resistance, and double-layer capacitance phenomena are represented by considering two series elements, composed by the parallel of resistance with an imperfect capacitance parameter, the so-called constant phase elements (CPEs). The introduction of a CPE improves the match between the fit and the experimental battery EIS measurement in frequency. In a parallel R-CPE circuit configuration, the transfer function is represented by the following formula:

$$Z_{R//CPE}(\omega) = \frac{R}{1 + RQ(\mathrm{j}\omega)^{\alpha}}$$

Equation 7-1

CPE includes two parameters: the capacitance parameter Q and the depression factor $\alpha \in [0,1]$. This last parameter allows the transfer function (Equation 7-1) to draw semi-ellipses arcs in Nyquist plots, which are fundamental to fit the battery impedance curve (Figure 8-1). More details about CPEs are shown in the previous work [12]. Finally, we consider the infinite Warburg element W to fit the impedance curve at the low-frequency band (diffusion process). The transfer function of the infinite Warburg element is similar to CPE [11], considering $\alpha = 0.5$ (in Nyquist diagram it means a bisector).

Given the Randles circuit model shown in Figure 7-1, the transfer function equation of battery impedance is according to:

$$Z_{battery}(\omega) = j\omega L + R_{\Omega} + \frac{R_{SEI}}{1 + (j\omega)^{\alpha_{SEI}}\tau_{SEI}} + \frac{R_{CT}}{1 + (j\omega)^{\alpha_{DL}}\tau_{CT,DL}} + \frac{1}{\sqrt{j\omega}Q_W}$$

Equation 7-2

Model parameters are identified by fitting experimental impedance data during EIS tests shown in the next sub-section. The model is non-linear in the parameters, hence, we apply the Levenberg-Marquardt algorithm, which is a non-linear best fitting algorithm.

7.2.4 Experimental EIS test description

The battery aged cells under the EIS test were presented and depicted in Section 4.2. All the EIS test measurements are executed in the UNIFI laboratories, by using the battery test bench shown in the previous works [8][13]. In [13], a low-cost and low-energy consumption hardware is presented to perform fast and accurate impedance identification in a wide frequency band. First simulations were performed in [14]. In this section, the several aged battery impedances are observed in the frequency band [0.45÷3500] Hz, exciting the battery at a rate of discharging current amplitude of C/3, measuring voltage and current at a sampling frequency 20 kHz. Moreover, surface and room temperature during the EIS test are measured every 1 s. Finally EIS test are performed at six various battery SOC (100%, 80%, 60%, 40%, 20% and 2%). An example of an EIS test in the range of SOC $[20 \div 80]$% is shown in Figure 7-2.

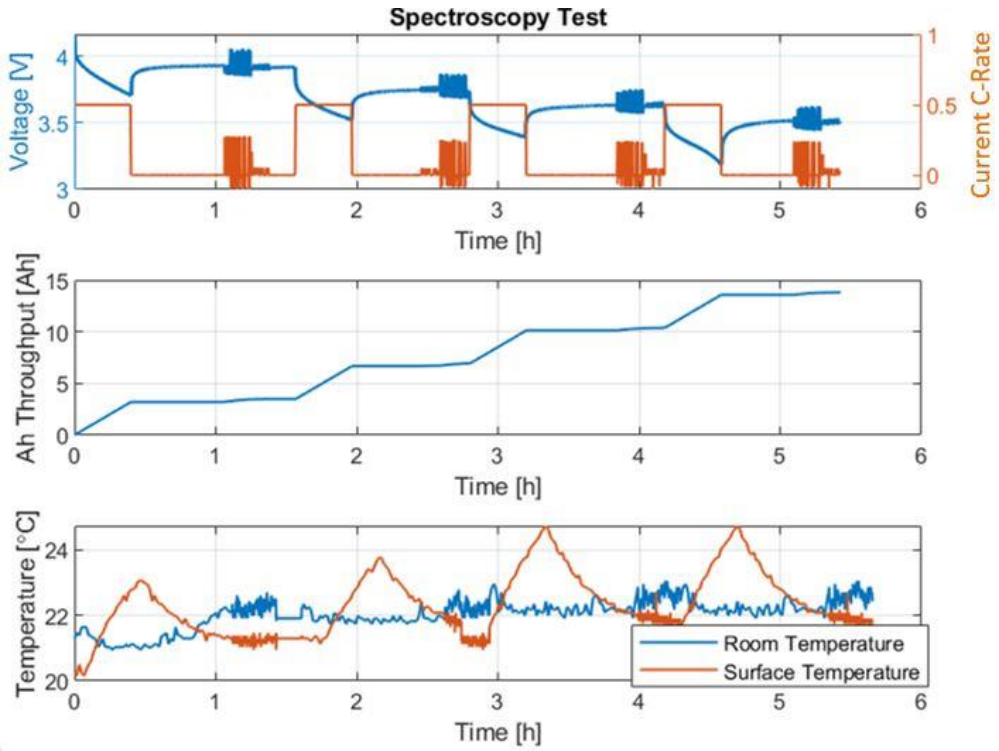

Figure 7-3: Sequence of EIS tests performed on an aged cell, interspersed by CC discharging at C/2 and rest time of 30 mins

7.2.5 EIS results

EIS tests are performed on EOL pouch NMC cells shown in section 4.2 in the frequency band [0.45,3500] Hz in the UNIFI laboratory [13]. Results are presented in Figure 7-3 for the cell at SOH=60%: six EIS tests are performed at different battery SOCs. We infer by results given in Figure 7-3 that there is a noticeable difference of real and imaginary part of impedance in low frequency at various SOC, especially at the highest and the lowest SOC. This observation is inferred also in the literature, concerning fresh batteries [15][16]. The novelty of this first analysis is that the growth of the SEI film during battery degradation becomes bigger respect to charge transfer resistance. In the literature, so for the EIS test of battery in the first life, the resistance value of the SEI is so small, in fact this impedance semi-circle arc is negligible [17].

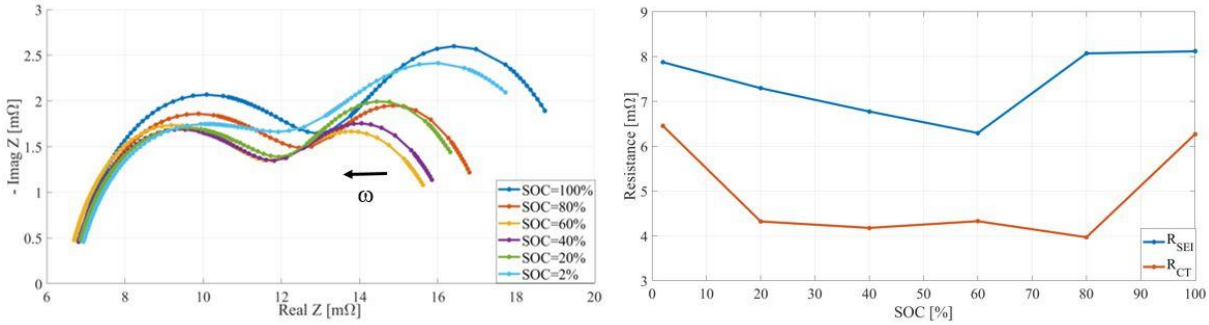

Figure 7-4: Measured battery impedance (SOH=60%) at various SOC: (a) Nyquist diagram, (b) SEI resistance and charge-transfer resistance evaluation

As mentioned in the section introduction, we will extrapolate many correlations between EIS results and SOH: in Figure 7-4 impedance curve is depicted for batteries at different SOHs (considering fixed SOC=60%). We notice a shift on the right of the impedance curve with aging. It means an increase of the real part of the impedance, i.e. an increase of static resistance of the battery with capacity degradation (SOH). This last consideration is also confirmed in literature previous research works [15]-[17] testing battery in the first life. The novelty of this second

analysis concerns the drastic increase of the two semi-ellipses arcs with aging, considering the EOL batteries under test. It means a drastic increase in charge-transfer resistance R_{CT} and SEI resistance R_{SEI}. All the EIS test and impedance measurement of the battery are considered: the circuit parameters depicted in Figure 7-1 are identified by fitting the impedance measurements with the transfer function (Equation 7-2). Results of parameter identification (resistance circuit elements) are shown in Figure 7-5. By the extraction of resistance parameters at various SOC and SOH, we infer that there is a noticeable increase of the ohmic resistance parameter R_{Ω} with battery aging, confirmed also in literature [15]-[17]. Observing the sum of the identified SEI and charge-transfer resistance parameters (Figure 7-5, $R_{SEI} + R_{CT}$), we notice a reliable correlation between SOH and impedance measurements. Indeed the curves of the identified parameters $R_{SEI} + R_{CT}$, in relation of SOC, are well-separated at various SOH. Hence, the last parameter, which describes the length of the two semi-ellipses diameters, is a candidate as a robust and reliable indicator of battery SOH. More discussions about the results are illustrated in [8].

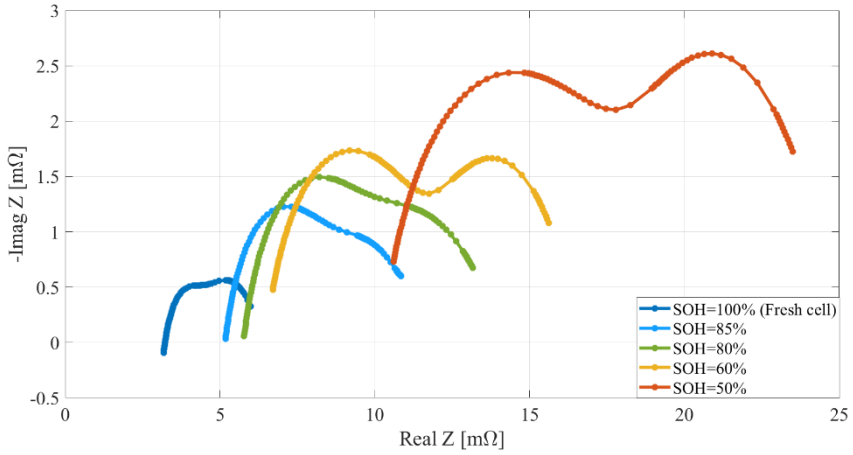

Figure 7-5: Battery impedance curve for NMC cell at different SOH (fixed SOC=60%)

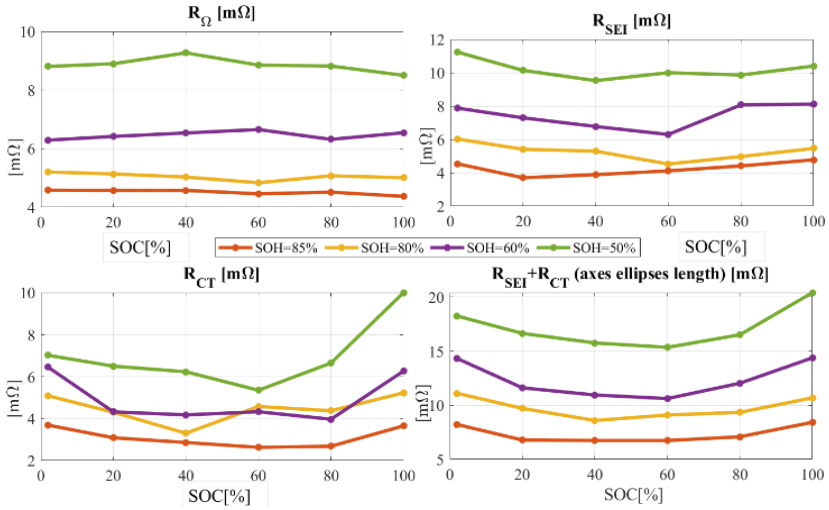

Figure 7-6: Resistance parameters extraction for EOL NMC cells at different SOC and SOH

7.2.6 Conclusions

EIS is a powerful method to investigate the state of health of lithium batteries. UNIFI has investigated the evolution of battery impedance with battery capacity degradation, evaluated by SOH indicator. Four EOL cells at different SOH are subjected to the EIS test in the frequency band [0.45÷3500] Hz.

Results of EIS tests confirm that the ohmic resistance of the battery increases with battery capacity degradation, during the second life. A drastic increase in the SEI resistance value is observed. Finally, a noticeable increase in the sum of SEI resistance and charge transfer resistance is evaluated. We infer by results that the degradation of the battery could be well correlated by using EIS tests, in particular, evaluating the SEI and charge transfer resistance parameters, which are defined, in this case study, in the frequency band about [10,2000] Hz. Fast and low-energy-consumption EIS tests in this frequency band can be performed by using low-cost hardware presented in [13].

7.3 Chapter references

[1] E. Hossain, D. Murtaugh, J. Mody, H. M. R. Faruque, M. S. H. Sunny, e N. Mohammad, «A Comprehensive Review on Second-Life Batteries: Current State, Manufacturing Considerations, Applications, Impacts, Barriers Potential Solutions, Business Strategies, and Policies», IEEE Access, vol. 7, pagg. 73215–73252, 2019, doi: 10.1109/ACCESS.2019.2917859.

[2] C. Zhang, J. Marco, e T. F. Yu, «Hardware Platform Design of Small Energy Storage System Using Second Life Batteries», in 2018 UKACC 12th International Conference on Control (CONTROL), set. 2018, pagg. 163–168, doi: 10.1109/CONTROL.2018.8516871.

[3] G. Barone et al., «CANOpen Communication of a 16.4kWh Li-ion Battery Energy Storage System for Nanogrids in Energy Community Framework», in 2019 9th International Conference on Power and Energy Systems (ICPES), dic. 2019, pagg. 1–6, doi: 10.1109/ICPES47639.2019.9105608.

[4] Berecibar, M., Gandiaga, I., Villarreal, I., Omar, N., Van Mierlo, J., & Van den Bossche, P. (2016). Critical review of state of health estimation methods of Li-ion batteries for real applications. Renewable and Sustainable Energy Reviews, 56, 572-587.

[5] Ceraolo, M., Giglioli, R., Lutzemberger, G., Langroudi, M. M., Poli, D., Andrenacci, N., & Pasquali, M. (2018, June). Experimental analysis of NMC lithium cells aging for second life applications. In 2018 IEEE International Conference on Environment and Electrical Engineering and 2018 IEEE Industrial and Commercial Power Systems Europe (EEEIC/I&CPS Europe) (pp. 1-6). IEEE.

[6] Watrin, N., Blunier, B., & Miraoui, A. (2012, June). Review of adaptive systems for lithium batteries state-of-charge and state-of-health estimation. In 2012 IEEE Transportation Electrification Conference and Expo (ITEC) (pp. 1-6). IEEE.

[7] Kim, I. S. (2009). A technique for estimating the state of health of lithium batteries through a dual-sliding-mode observer. IEEE Transactions on Power Electronics, 25(4), 1013-1022.

[8] Locorotondo, E., Cultrera, V., Pugi, L., Berzi, L., Pierini, M., Pasquali, M., Andrenacci, N., Lutzemberger, G., "Impedance spectroscopy characterization of lithium batteries with different ages in second life application", In 2020 IEEE International Conference on Environment and Electrical Engineering and 2020 IEEE Industrial and Commercial Power Systems Europe, in press.

[9] L. Ljung, ”System Identification - Theory for the User”, Prentice Hall, 1999.

[10] Randles, J. E. B. (1947). Kinetics of rapid electrode reactions. Discussions of the faraday society, 1, 11-19.

[11] F. Berthier, J.P Diard, R. Michel, "Distinguishability of equivalent circuits containing CPEs: Part I. Theoretical part." Journal of Electroanalytical Chemistry, 510(1-2), 1-11, 2001.

[12] Locorotondo, E., Pugi, L., Berzi, L., Pierini, M., Scavuzzo, S., Ferraris, A., ... & Carello, M. (2019, September). Modeling and simulation of Constant Phase Element for battery Electrochemical Impedance Spectroscopy. In 2019 IEEE 5th International forum on Research and Technology for Society and Industry (RTSI) (pp. 225-230). IEEE.

[13] Serni, T., Locorotondo, E., Pugi, L. Berzi, L. Pierini, M., & Cultrera, V. (2020). A Low Cost Programmable Hardware for Online Spectroscopy of Lithium Batteries. In 2020 IEEE Mediterranean Electrotechnical Conference (MELECON), in press.

[14] Locorotondo, E., Scavuzzo, S., Pugi, L., Ferraris, A., Berzi, L., Airale, A., ... & Carello, M. (2019, June). Electrochemical Impedance Spectroscopy of Li-Ion battery on-board the Electric Vehicles based on Fast nonparametric identification method. In 2019 IEEE International Conference on Environment and Electrical Engineering and 2019 IEEE Industrial and Commercial Power Systems Europe (EEEIC/I&CPS Europe) (pp. 1-6). IEEE.

[15] Andre, D., Meiler, M., Steiner, K., Wimmer, C., Soczka-Guth, T., & Sauer, D. U. (2011). Characterization of high-power lithium-ion batteries by electrochemical impedance spectroscopy. I. Experimental investigation. Journal of Power Sources, 196(12), 5334-5341.
[16] De Sutter, L., Firouz, Y., De Hoog, J., Omar, N., & Van Mierlo, J. (2019). Battery aging assessment and parametric study of lithium-ion batteries by means of a fractional differential model. Electrochimica Acta, 305, 24-36.
[17] Olofsson, Y., Groot, J., Katrašnik, T., & Tavčar, G. (2014, December). Impedance spectroscopy characterisation of automotive NMC/graphite Li-ion cells aged with realistic PHEV load profile. In 2014 IEEE International Electric Vehicle Conference (IEVC) (pp. 1-6). IEEE.

8 Life cycle assessment of second life batteries (LCA)

8.1 Production impact of Lithium batteries

The LCA of the batteries is carried out based on Ecoinvent 3.1 database (2009-2010). The environmental impacts are expressed in terms of Global Warming Potential, since it is by far the most often studied LCIA category. The chosen functional unit is the total mean GHG emissions associated with the production of 1 kWh of storage capacity or 1 kg of battery. Ecoinvent database attributes to a generic Li-ion battery production an emission equal to 183 kg CO_{2eq}/kWh (22 kgCO_{2eq}/kg batt). To verify the affordability of Ecoinvent secondary data, the obtained results are compared with recent literature sources. Numerous studies on the potential environmental impacts of LIB production exist, however these are heterogeneous and therefore the comparability is limited. After a thorough review of numerous publications, a total of 15 LCA studies dealing with battery production are identified, that fulfil the selection criteria (e.g. providing detailed results for LIB production and disclosing sufficient information to calculate impacts per battery kg or kWh storage capacity). The results of literary review are reported in Table 8-1, including the comparison with the impacts obtained in OBELICS.

Table 8-1: Production impacts for different Li-ion batteries

Studies	Type of battery	kgCO^2eq/kWh	kg CO^2eq/kg batt
Notter et al., 2010	LMO	55	6.3
Dunn et al., 2012		40	4.6
EPA, 2013		62	7.1
Hao et al., 2017		97	11.1
Kim et al., 2016	LMO-NMC	140	15.4
Majeau-Bettez et al., 2011		200	22
EPA, 2013		120	13.2
Ellingsen et al., 2014		172	18.9
Hao et al., 2017		104	11.4
Philippot et al., 2018		163	17.9
Majeau-Bettez et al., 2011	LFP	250	25
EPA, 2013		152	15.2
Hao et al., 2017		115	11.5
Raugei et al., 2019	LCP	76	19
Philippot et al., 2018	NCA	123	23.4
GaBi-Ecoinvent 3.1	generic Li-ion	183	22

The studies from literature assess different battery chemistries. In particular cathode chemistries include: manganese spinel oxide (LMO) and composite oxide including nickel, cobalt, aluminum (NMC, NCA), lithium iron phosphate (LFP) and lithium cobalt phosphate (LCP). For each battery chemistries articles analyzed are ordered increasingly in a temporal order. Results vary from 55 to 250 kg CO_2eq/kWh, with a mean value of 124 kg CO_2eq/kWh. Variability of the results is associated with numerous factors. Physical size and structure of battery pack determinate variations in the assumed relative mass shares of non-electrochemical components which reflect on the calculated impacts per kWh of battery energy capacity. Furthermore, the assumed electricity grid mixes and their associated carbon intensities have a potentially large effect on results. The cathode composition appears to have a distinctive effect on the outcome. Within each family of cathode chemistries, there are some indications of a general downward trend with time, albeit with the possible exception of LMO batteries.

8.2 Production impact of other battery type alternative to second-life battery

The purpose of this study is to analyze the environmental impacts of the reuse of electric vehicle Li-ion batteries in stationary energy storage. The environmental feasibility criterion is defined by an equivalent-functionality Pb battery. In fact, the Pb battery is a widely used incumbent technology for stationary purposes due to its affordability.
Concerning the Pb batteries, the LCI has be modelled based on Ecoinvent DB. The GWP associated with the production stage is 71 kg CO^2eq/kWh (2.7 kg CO^2eq/kg batt). The reliability of this result is verified through comparison with literature data (Table 2).

Table 8-2: Production impacts for Pb batteries

Studies	Type of battery	kgCO2eq/kWh	kg CO2eq/kg batt
Rydh et al., 2005	Pb	81	3.1
Greet 2.7, 2007		168	6.4
Manus et al., 2012		23.7	0.9
Liu et al., 2015		101.4	3.9
Davidson et al., 2016		33	1.3
GaBi-Ecoinvent 3.1		71	2.7

Existing studies assess the GWP of Pb battery production within 24-100 kg CO2 eq/kWh. As a consequence, the result obtained in Obelics is perfectly in line with literature works. The only exception is Greet 2.7 (2007) which provides an impact of 168 kgCO2eq/kWh; however, the study can be considered outdated since it is more than 10 years old.

8.3 Repurposing and Recycling impact

Usually an electric vehicle battery is degraded when it has about 80% of its initial capacity. The repurposing process is functional to extend the life of an electric vehicle battery pack with a cascading second phase use. The aim of the repurposing is to refurbish the battery pack (modifying cathode, anode and electrolyte), so that battery is able to providing a 5 years additional life span. After the removal from the electric vehicle the battery pack is disassembled into modules. Subsequently, the modules are inspected and tested to determine the working conditions and electric performance. The re-purposed module undergoes re-assembly of cells and modules into packs, and the installation of a new battery management system suitable for the new second use application and new operation conditions.
In OBELICS, the environmental impacts of the repurposing are assessed in terms of GWP and it is assumed as 10 % of the production phase. Table 8-3 reports a literature review regarding the GWP of production and re-purposing for different typologies of batteries.

Table 8-3: Production and repurposing impacts for different Li-ion batteries

Studies	Type of battery	Production		Repurposing		%
		$kgCO_2eq/kWh$	$kgCO_2eq/kg$ batt	$kgCO_2eq/kWh$	$kgCO_2eq/kg$ batt	
Bobba et al., 2018	LMO-NMC	242	26.6	7.7	0.8	3
Kannangara, 2018	NMC	147.1	25.0	6	0.9	4
Ahmadi et al., 2014	generic Li-ion	120	12	60	6	50
Richa et al., 2017	LMO	59	6.7	66	7.5	112
GaBi-Ecoinvent 3.1	generic Li-ion	183	22	18	2.16	10

Results are very heterogeneous:

- Bobba et al. and Kannangara et al. assess the repurposing impact 3-4 % lower than the production phase;
- Ahmadi et al. estimates the repurposing GWP approximated as half of manufacturing;
- Richa et al. states that the impact of repurposing is higher than the production, thus leading to the conclusion that it is not convenient from an environmental point of view.

The conducted LCA assumes that the EoL battery is properly collected and forwarded to recycling. Li-ion batteries consist of battery cells containing electrolyte, separator cathode and anode. Various types of lithium-ion battery are available (LFP, LMO, NMC, NCA,..): each of these results in different battery properties and characteristics, making them suitable for different recycling processes. For material recovery from Li-ion batteries, chemical processes and "direct recycling" procedures are a viable solution. The chemical metal extraction methods can be divided into two main types, which are pyrometallurgical and hydrometallurgical treatments.
The LCI for the recycling process is performed based on the Ecoinvent database for the pyrometallurgical and hydrometallurgical processes: the analysis assesses only positive impacts (environmental burdens) of recycling processes, without considering credits due to lack of inventory data. The results obtained are compared with other literature studies (Table 8-4).

Table 8-4: Production and end of life impacts for different Li-ion batteries

Studies	Type of battery		Production		EoL						
			$kgCO_2eq/kWh$	$kgCO_2eq/kg$ batt	Rec proc	impact	credit	net imp	impact	credit	net imp
						$kgCO_2eq/kWh$			$kgCO_2eq/kg$ batt		
Bobba et al., 2018	LMO-NMC		242	37.5	pyrom	NA	NA	-15.6	NA	NA	-2.4
Ciez et al., 2019	NMC	pouch battery	99	10.9	pyrom	86.4	70.0	16.4	9.5	7.7	1.8
					hydrom	68.2	71.8	-3.6	7.5	7.9	-0.4
					direct	72.7	85.5	-12.7	8.0	9.4	-1.4
		cylindrical battery	45	9.0	pyrom	60.5	58.0	2.5	12.1	11.6	0.5
					hydrom	49.0	53.0	-4.0	9.8	10.6	-0.8
					direct	40.0	42.5	-2.5	8.0	8.5	-0.5
	NCA	pouch battery	47.5	9.0	pyrom	43.7	37.4	6.3	4.8	4.1	0.7
					hydrom	41.6	41.8	-0.3	4.6	4.6	0.0
					direct	42.1	48.4	-6.3	4.6	5.3	-0.7
		cylindrical battery	44	8.4	pyrom	63.2	62.1	1.1	12.6	12.4	0.2
					hydrom	51.6	54.7	-3.2	10.3	10.9	-0.6
					direct	41.6	43.2	-1.6	8.3	8.6	-0.3
	LFP	pouch battery	63	6.3	pyrom	81.0	63.0	18.0	8.9	6.9	2.0
					hydrom	80.0	64.0	16.0	8.8	7.0	1.8
					direct	85.0	78.0	7.0	9.4	8.6	0.8
		cylindrical battery	78	7.8	pyrom	79.0	69.0	10.0	15.8	13.8	2.0
					hydrom	78.0	70.0	8.0	15.6	14.0	1.6
					direct	74.0	59.0	15	14.8	11.8	3.0
Cusenza et al., 2019	LMO-NMC		312.4	48.4	pyrom	16.3	31.6	-15.3	2.5	4.9	-2.4
Raugei et al., 2019	LCP		76.1	7.6	hydrom	5.8	11.2	-5.4	0.6	1.1	-0.5
Richa et al., 2017	LMO		59	6.7	mix pyr-hyd	66	78.5	-12.5	7.5	8.9	-1.4
GaBi-Ecoinvent 3.1	generic Li-ion		183	22	pyrom	22.5	NA	NA	2.7	NA	NA
					hydrom	30	NA	NA	3.6	NA	NA

For 12 studies the beneficial effect of recycling overcomes the impacts, thus resulting in an overall environmental credits; on the other hand, for the remaining researches the impacts of recycling processes are not counterbalanced by credits.

Concerning Pb batteries, the approximate recycling rate is about 98 %. The recycling of Pb battery involves a smelter based process for secondary lead production. Recycling credit is provided thanks to the avoided production of virgin lead, according to the initial fraction of lead primary and secondary sources. Table 8-5 reports results of two studies from literature dealing with recycling processes of lead batteries.

Table 8-5: End of life impacts for Pb batteries

Studies	Type of battery	kgCO_2eq/kWh	kg CO_2eq/kg batt
Liu et al., 2015	Pb	-47.3	-1.8
Richa et al., 2017		-31.6	-1.2

8.4 Use phase

Bobba et al. provides a case study similar to the OBELICS application, that is the use of repurposed batteries to increase photovoltaic self-consumption in a given dwelling. The calculation of use stage impacts requires an assessment of the energy flows which characterize the system in which the battery is used, according to the battery characteristics and system configuration. The input/output energy flows (E_{in} and E_{out}) consist in home, PV and battery (Figure 8-1).

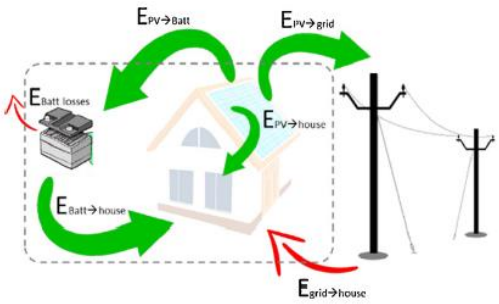

$E_{PV\rightarrow Batt}$ = energy provided to the battery from the PV installation
$E_{PV\rightarrow grid}$ = energy provided to the grid from the PV installation
$E_{Batt\ losses}$ = energy lost due to the battery efficiency
$E_{PV\rightarrow house}$ = energy provided to the house from the PV installation
$E_{Batt\rightarrow house}$ = energy provided to the house from the battery
$E_{grid\rightarrow house}$ = energy required by the house from the grid

$$E_{in} = E_{PV\rightarrow grid} = E_{requirement} - E_{PV\rightarrow house} - E_{PV\rightarrow Batt}$$
$$E_{out} = E_{grid\rightarrow house} = E_{requirement} - E_{PV\rightarrow house} - E_{Batt\rightarrow house}$$

Figure 8-1: Energy flows of the system (Bobba et al.)

All system energy flows are calculated every 15 min for 1 year. The model assumes that the depth of battery discharge does not exceed 80 % and the efficiency is assumed to linearly decrease by 5 % points in 5 years. The model is run until the battery capacity reaches 60 % of its nominal capacity; if the capacity is lower, the battery should be discarded. The study assesses a comparison of different scenarios from a life cycle perspective. The reference scenario assumes that a fresh battery is used in a storage application after which it is recycled. The repurposed scenario relates to all LC stages involved in the second use. The input/output energy flows for each scenario are shown in Table 8-6.

Table 8-6: Energy flows for the reference and the repurposed scenarios (Bobba et al.)

Parameter	Reference scenario A	Reference scenario B	Reference scenario C	Repurposed scenario
Lifetime [years]	7.4	1	1	3.6
Electricity required by house [kWh]	38.1	5.1	5.1	18.4
Direct electricity consumption from PV [kWh]: $E_{PV\rightarrow house}$	12.4	1.7	1.7	6.0
Electricity provided by batteries [kWh]: $E_{Batt\rightarrow house}$	11.1	-	-	5.1

Electricity needed for charging batteries [kWh]: $E_{PV \rightarrow Batt}$	11.7	-	-	5.5
Electricity from the grid [kWh]: E_{out} = $E_{grid \rightarrow house}$	14.6	3.5	3.5	7.3
PV production [kWh]	35.7	4.8	4.8	17.3
Electricity potentially to be fed into the grid [kWh]: $E_{in} = E_{PV \rightarrow grid}$	11.6	3.2	-	5.8

The results suggest that the repurposed battery can be used 3.6 years before its capacity reaches 60 % of its nominal capacity, the fresh battery lifetime being about 7.4 years.
Richa et al. is another work comparable with the OBELICS case study. One of the purposes of this article is to compare the environmental impacts of a stationary energy storage system based on refurbished electric vehicle lithium-ion batteries with an equivalent lead acid battery-based system. An energy storage system is considered from the perspective of a utility operator facing the choice of either using a refurbished Li-ion battery or a new PbA battery system. Thus an equivalent functionality PbA battery based storage system is used as a basis for comparison. Figure 3 illustrates the analyzed LC stages for both Li-ion (a) and PbA (b) system.

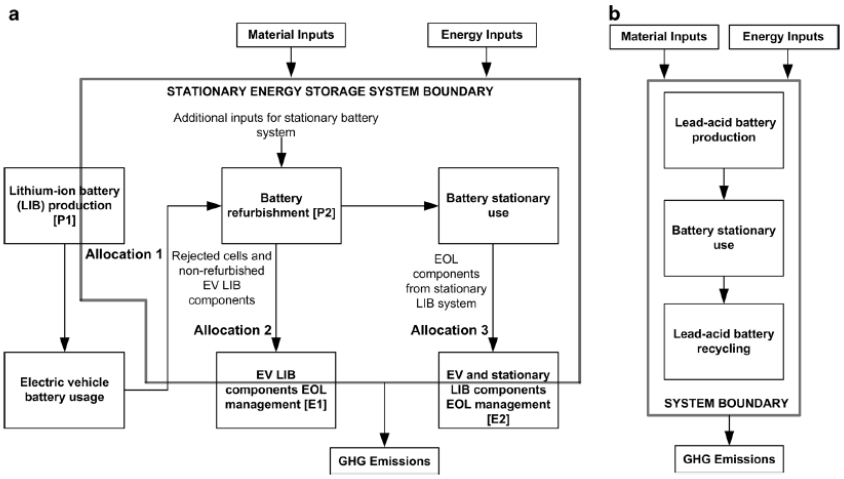

Figure 8-2: System boundary to compare environmental implications of battery choice for stationary energy storage (Richa et al.)

The electric vehicle use phase is modelled as lost in electricity due to battery efficiency decrease over car life-time and the additional energy needed to carry the weight of the battery. In early life, a 95 % roundtrip efficiency is assumed using data from vehicle tests for the Nissan LEAF battery. The EoL battery efficiency is assumed 80 %. In addition to electricity consumption, the use phase also includes battery transport from the manufacturer to the car assembly site. For the stationary energy storage case, it is assumed that both Li-ion and PbA batteries have a 450 kWh energy storage. Both batteries deliver 150 kWh every day. This value is calculated for each cycle by adjusting the depth of discharge (which is in the range 33-42 %) as the batteries aged. At the end of first life both nominal and peak power capability of EV LIB is expected to decrease by at least 25 % from its initial value. The PbA battery has a nominal power rating of 50 kW. For this type of battery, it is assumed that the increase in battery internal resistance and efficiency losses occurs over time. The efficiency of PbA battery generally lies between 70% and 85%. Unlike LIBs, PbA batteries do no start with their peak capacity, but rather at a lower capacity at the beginning of life and their capacity increases with aging. The PbA battery capacity is modeled to reduce linearly by a constant of approximately 0.05 over its 5 year lifespan. For estimating electricity losses due to PbA battery efficiency over its lifespan, an assumption of 25% increase in resistance and hence a 25% increase in efficiency loss at battery end of life is made. Moreover, this assumption represents the worst case for LIBs when compared with lead-acid batteries.

9 Conclusions on second life battery applications

Finding applications for used batteries is expected to gain further interest in the future due to possibility to reduce the competition between emerging sectors (energy for industry, for residential use, and automotive field) while providing prolongation of use for existing components, thus reducing of the pressure on manufacturers, mining activities and raw material sector, as shown by literature studies.

The activities here shown as been structured in order to provide a comprehensive overview on the application of second life battery.
Looking at cell analysis, a testing procedure has been applied comprehending both capacity testing and impedance spectroscopy testing with the aim of:

- Ensuring that used cells are usable with sufficient efficiency in applications other than automotive, which is verified for moderate and small currents
- Implement the knowledge on battery cells in a reusable Simulink model
- Suggest diagnostics methodologies for further in service or repurposing diagnostics.

Looking at application analysis, at least two case studies have been suggested for which the application of battery can provide in use advantages:

- Relevant energy saving, that is the case of tramway applications for regenerated energy harvesting
- Relevant energy optimization (in terms of economic and environmental indications), if energy storage is coordinated with a plant comprehending statistically partially predictable production and energy use.
- A new indicator of battery economic and environmental performances has been adopted.

Looking at the environmental impact related to battery production, the wide literature available has been consulted together with a comparison with environmental impact databases for LCA. It emerged that due to the number of different approaches, indicators, functional units adopted, a strong concordance between the sources has not emerged. However, it is confirmed that considering prolongation of use of Li-Ion batteries through repurposing is, according to most authors, not only preferable to the use of new li based batteries but also often convenient in comparison with other suitable technologies such as the still used Lead-based batteries for stationary applications.

10 Acknowledgement

The author(s) would like to thank the partners in the project for their valuable comments on previous drafts and for performing the review.

Project partners:

Partner no.	Partner organisation name	Short Name
1	AVL List GmbH	AVL
2	Centro Richerche Fiat SCpA	CRF
3	FORD Otomotiv Sanayi Anonim sirketi	FO
4	Renault Trucks SAS	RT-SAS
5	AVL Software and Functions GmbH	AVL-SFR
6	Robert Bosch GmbH	Bosch
7	SIEMENS INDUSTRY SOFTWARE NV	SIE-NV
8	SIEMENS Industry Software SAS	SIE-SAS
9	Uniresearch BV	UNR
10	Valeo Equipements Electroniques Moteurs	Valeo
11	Commissariat à l'Energie Atomique et aux Energies Alternatives	CEA
12	LBF Fraunhofer	FhG-LBF
13	FH Joanneum Gesellschaft M.B.H.	FHJ
14	National Institute of Chemistry	NIC
15	University Ljubljana	UL
16	University Florence	UNIFI
17	University of Surrey	US
18	Das Virtuelle Fahrzeug Forschungsgesellschaft mbH	VIF
19	Vrije Universiteit Brussel	VUB

This project has received funding from the European Union's Horizon 2020 research and innovation programme under grant agreement No 769506.